Inorg. Chem. **2004**, *43*, 757–777

Structural, NMR, and EPR Studies of $S = {}^1/_2$ and $S = {}^3/_2$ Fe(III) Bis(4-Cyanopyridine) Complexes of Dodecasubstituted Porphyrins

Liliya A. Yatsunyk and F. Ann Walker*

Department of Chemistry, University of Arizona, Tucson, Arizona 85721-0041

Received August 27, 2003

The NMR and EPR spectra for three complexes, iron(III) octamethyltetraphenylporphyrin bis(4-cyanopyridine) perchlorate, [FeOMTPP(4-CNPy)$_2$]ClO$_4$, and its octaethyl- and tetra-β,β'-tetramethylenetetraphenylporphyrin analogues, [FeOETPP-(4-CNPy)$_2$]ClO$_4$ and [FeTC$_6$TPP(4-CNPy)$_2$]ClO$_4$, are presented. The crystal structures of two different forms of [FeOETPP-(4-CNPy)$_2$]ClO$_4$ and one form of [FeOMTPP(4-CNPy)$_2$]ClO$_4$ are also reported. Attempts to crystallize [FeTC$_6$TPP-(4-CNPy)$_2$]ClO$_4$ were not successful. The crystal structure of [FeOMTPP(4-CNPy)$_2$]ClO$_4$ reveals a saddled porphyrin core, a small dihedral angle between the axial ligand planes, 64.3°, and an unusually large tilt angle (24.4°) of one of the axial 4-cyanopyridine ligands with respect to the normal to the porphyrin mean plane. There are 4 and 2 independent molecules in the asymmetric units of [FeOETPP(4-CNPy)$_2$]ClO$_4$ crystallized from CD$_2$Cl$_2$/dodecane (**1**–**4**) and CDCl$_3$/cyclohexane (**5**–**6**), respectively. The geometries of the porphyrin cores in **1**–**6** vary from purely saddled to saddled with 15% ruffling admixture. In all structures, the Fe–N$_p$ distances (1.958–1.976 Å) are very short due to strong nonplanar distortion of the porphyrin cores, while the Fe–N$_{ax}$ distances are relatively long (~2.2 Å) compared to the same distances in $S = {}^1/_2$ bis(pyridine)iron(III) porphyrin complexes. An axial EPR signal is observed ($g_\perp = 2.49$, $g_{||} = 1.6$) in frozen solutions of both [FeOMTPP(4-CNPy)$_2$]ClO$_4$ and [FeTC$_6$TPP(4-CNPy)$_2$]ClO$_4$ at 4.2 K, indicative of the low spin (LS, $S = {}^1/_2$), $(d_{yz}d_{xz})^4(d_{xy})^1$ electronic ground state for these two complexes. In agreement with a recent publication (Ikeue, T.; Ohgo, Y.; Ongayi, O.; Vicente, M. G. H.; Nakamura, M. *Inorg. Chem.* **2003**, *42*, 5560–5571), the EPR spectra of [FeOETPP-(4-CNPy)$_2$]ClO$_4$ are typical of the $S = {}^3/_2$ state, with g values of 5.21, 4.25, and 2.07. A small amount of LS species with $g = 3.03$ is also present. However, distinct from previous conclusions, large negative phenyl-H shift differences $\delta_m - \delta_o$ and $\delta_m - \delta_p$ in the ^{1}H NMR spectra indicate significant negative spin density at the *meso*-carbons, and the larger than expected positive average CH$_2$ shifts are also consistent with a significant population of the $S = 2$ Fe(II), $S = {}^1/_2$ porphyrin π-cation radical state, with antiferromagnetic coupling between the metal and porphyrin unpaired electrons. This is the first example of this type of porphyrin-to-metal electron transfer to produce a partial or complete porphyrinate radical state, with antiferromagnetic coupling between metal and macrocycle unpaired electrons in an iron porphyrinate. The kinetics of ring inversion were studied for the [FeOETPP(4-CNPy)$_2$]ClO$_4$ complex using NOESY/EXSY techniques and for the [FeTC$_6$TPP(4-CNPy)$_2$]ClO$_4$ complex using DNMR techniques. For the former, the free energy of activation, $\Delta G^\ddagger$, and rate of ring inversion in CD$_2$Cl$_2$ extrapolated to 298 K are 63(2) kJ mol^{-1} and 59 s^{-1}, respectively, while for the latter the rate of ring inversion at 298 K is at least 4.4×10^7 s^{-1}, which attests to the much greater flexibility of the TC$_6$TPP ring. The NMR and EPR data are consistent with solution magnetic susceptibility measurements that show $S = {}^3/_2$ in the temperature range from 320 to 180 K for [FeOETPP(4-CNPy)$_2$]$^+$, while both [FeOMTPP(4-CNPy)$_2$]$^+$ and [FeTC$_6$TPP(4-CNPy)$_2$]$^+$ change their spin state from $S = {}^3/_2$ at room temperature to mainly LS ($S = {}^1/_2$) upon cooling to 180 K.

Introduction

Iron(III) porphyrinate complexes with very weakly basic ligands have been investigated for some time, and a variety of magnetic and structural behavior has been reported. On the basis of previous studies of [FeOEP(L)$_2$]$^+$ with various pyridines, it was found that complexes with strongly basic pyridines (pK_a(BH$^+$) > 8) are low spin, LS, with the $(d_{xy})^2(d_{xz},d_{yz})^3$ electronic ground state,[1,2] while on the other hand, complexes with very weakly basic pyridine ligands (pK_a(BH$^+$) < 3) have an admixed intermediate-spin, IS, state ($S = {}^3/_2, {}^5/_2$),[3] and even in one case a thermal spin equilibrium ($S = {}^1/_2 \leftrightarrow S = {}^5/_2$).[4] For example, [FeOEP(3-ClPy)$_2$]ClO$_4$ (pK_a(PyH$^+$) = 2.83) gives both IS and spin equilibrium states, depending on the crystal lattice,[4] and [FeOEP(3,5-

* To whom correspondence should be addressed. E-mail: awalker@u.arizona.edu.

(1) Innis, D.; Soltis, S. M.; Strouse, C. E. *J. Am. Chem. Soc.* **1988**, *110*, 5644−5650.
(2) Walker, F. A.; Reis, D.; Balke, V. L. *J. Am. Chem. Soc.* **1984**, *106*, 6888−6898.
(3) Scheidt, W. R.; Osvath, S. R.; Lee, Y. J.; Reed, C. A.; Shaevitz, B.; Gupta, G. P. *Inorg. Chem.* **1989**, *28*, 1591−1595.
(4) Safo, M. K.; Scheidt, W. R.; Gupta, G. P.; Orosz, R. D.; Reed, C. A. *Inorg. Chim. Acta* **1991**, *184*, 251−258.

10.1021/ic035010q CCC: $27.50
Published on Web 12/23/2003

$Cl_2Py)_2]ClO_4$ is in a discrete admixed IS state.[3] When $[FeTMP(L)_2]^+$ and $[FeTPP(L)_2]^+$ complexes are considered, all of them are LS, regardless of the basicity of the axial pyridine, and specifically, complexes with weakly basic pyridines are LS with the $(d_{xz},d_{yz})^4(d_{xy})^1$ electronic ground state.[5,6]

The structures of $[FeTPP(4\text{-}CNPy)_2]ClO_4$ and $[FeTMP(L)_2]ClO_4$ with L = 3-ClPy and 4-CNPy have strongly S_4-ruffled distortion of the porphyrin core.[5,6] The axial ligands are held in perpendicular planes over the *meso* positions (the observed φ angle[7] ranges from 29° to 48°).[5,6] It is interesting to note that $[FeTPP(4\text{-}CNPy)_2]ClO_4$ has the most extensively ruffled porphyrin core among any of the bis(pyridine) iron(III) porphyrinates, which is manifested by a large deviation of the *meso*-carbons from the mean plane (±0.55 Å), as well as by strong twisting of the pyrrole rings.[6] EPR spectra of the Fe(III)TMP complexes with strongly and moderately basic pyridines (4-Me_2NPy, 4-NH_2Py, and 3-EtPy) and even with 3-ClPy consist of single-feature "large g_{max}" signals with g values ranging from 3.40 to as low as 2.89, which are indicative of the low spin $(d_{xy})^2(d_{xz},d_{yz})^3$ electronic ground state.[5] On the other hand, the EPR spectra of bis(4-cyanopyridine) iron(III) complexes with various porphyrin ligands, TMP, TPP, T^nPrP, T^cPrP, T^iPrP, and OMTPP, exhibit axial EPR spectra with $g_\perp > 2 > g_\parallel$.[5,6,8−10] The analysis of these g values in the "proper axis system" of Taylor[11] indicates a shift in electronic ground state from $(d_{xy})^2(d_{xz},d_{yz})^3$ to a predominantly $(d_{xz},d_{yz})^4(d_{xy})^1$ configuration as the basicity of the pyridine is lowered. The change in electronic ground state was attributed to the stabilization of the filled d_{xz},d_{yz} orbitals of the iron by (d_π)Fe → L(π^*) back-donation due to the π-acceptor ability of the 4-CNPy ligand.[6] In addition, and probably more important, the low basicity of this pyridine toward the proton ($pK_a(PyH^+) \sim 1.1$[5,12]) leads to its being an extremely weak σ-donor to Fe(III) as compared to the porphyrin ring, which can also stabilize the d_{xz},d_{yz} orbitals relative to the in-plane d_{xy} metal orbital.

The two different electron configurations of low-spin Fe(III) porphyrinates result in different patterns of spin delocalization, as shown by the proton NMR spectra of representative complexes: in the case of the more common ground state, $(d_{xy})^2(d_{xz},d_{yz})^3$, there is large spin density at the pyrrole-β positions and little or no spin density at the porphyrin *meso*-carbons,[13−15] whereas in the case of the less common ground state, $(d_{xz},d_{yz})^4(d_{xy})^1$, negligible spin delocalization occurs to the pyrrole-β positions and large spin delocalization occurs to the porphyrin *meso* positions.[14−16] The reason for the latter is believed to be that the half-filled d_{xy} orbital can participate in strong porphyrin → Fe π donation from the filled $3a_{2u}(\pi)$ porphyrin orbital *if and only if* the porphyrinate ring ruffles strongly, leading to at least a 15° twist of nitrogen p_z orbitals away from the heme normal so that there is a significant p_z component in the *xy* plane.[6] It is thus porphyrin → Fe π donation that is believed to stabilize the ruffled conformation of porphyrin complexes that have the $(d_{xz},d_{yz})^4(d_{xy})^1$ electron configuration; this mechanism is not available to low spin d^6 Fe(II) porphyrinates, and thus the same ligands that stabilize the $(d_{xz},d_{yz})^4(d_{xy})^1$ electron configuration and have very ruffled porphyrinate cores and perpendicular axial ligand planes for low spin Fe(III) have planar porphyrinate cores and parallel axial ligand planes for low spin Fe(II).[17]

Octaalkyltetraphenylporphyrins such as OETPP are of great interest because they combine the peripheral substituents from both OEP and TPP, which results in a new geometry ($FeOEPL_2^+$ complexes are usually close to planar, the TPP analogues are S_4-ruffled and the OETPP analogues are for the most part saddled[18]) and, therefore, different spectroscopic properties. Investigation of highly nonplanar S_4-saddled (OETPP) and S_4-ruffled (T^iPrP) iron(III) porphyrin complexes with weakly coordinated axial ligands (THF, 4-CNPy, Py) has resulted in three recent communications by Nakamura et al.[19−21] that have been interpreted as showing that these complexes have very pure intermediate spin state. The major reasons were suggested to be (1) the short Fe−N_p bond length commonly observed in highly deformed porphyrin complexes; and (2) the weak coordinating ability of the axial ligands. The first point was supported by obtaining the crystal structure of $[FeT^iPrP(THF)_2]ClO_4$. The average Fe−N_p distance of 1.967(12) Å is significantly shorter than the same distances in the other bis(tetrahydrofuran)iron(III) porphyrin complexes (1.994, 2.006, and 2.016 Å for $[FeOEP(THF)_2]ClO_4$, $[FeTEtP(THF)_2]ClO_4$, and $[FeTPP(THF)_2]ClO_4$, respectively).[22−24] In the case of both strongly

(5) Safo, M. K.; Gupta, G. P.; Watson, C. T.; Simonis, U.; Walker, F. A.; Scheidt, W. R. *J. Am. Chem. Soc.* **1992**, *114*, 7066−7075.
(6) Safo, M. K.; Walker, F. A.; Raitsimring, A. M.; Walters, W. P.; Dolata, D. P.; Debrunner, P. G.; Scheidt, W. R. *J. Am. Chem. Soc.* **1994**, *116*, 7760−7770.
(7) The φ angle is defined as the angle between the projection of planar axial ligand onto the porphyrin mean plane and the closest N_P−Fe−N_P vector. It can also be defined as the dihedral angle between the axial ligand plane and the plane formed by Fe, two opposite Ns of the porphyrin core, and two ligand nitrogens that are coordinated to Fe(III). It is expected to be close to 45° for ideal ruffled geometry of the porphyrin core and 0−10° for ideal saddled porphyrin cores with perpendicular orientation of axial ligands in both cases.
(8) Ikeue, T.; Ohgo, Y.; Saitoh, T.; Nakamura, M.; Fujii, H.; Yokoyama, M. *J. Am. Chem. Soc*. **2000**, *122*, 4068−4076.
(9) Ikeue, T.; Ohgo, Y.; Saitoh, T.; Yamaguchi, T.; Nakamura, M. *Inorg. Chem.* **2001**, *40*, 3423−3434.
(10) Ikeue, T.; Ohgo, Y.; Ongayi, O.; Vicente, M. G. H.; Nakamura, M. *Inorg. Chem.* **2003**, *42*, 5560−5571.
(11) Taylor, C. P. S. *Biochim. Biophys. Acta* **1977**, *491*, 137−149.
(12) Hansch, C.; Leo, A.; Taft, R. W. *Chem. Rev.* **1991**, *91*, 165−195.
(13) La Mar, G. N.; Walker, F. A. *J. Am. Chem. Soc.* **1973**, *95*, 1782−1790.
(14) Walker, F. A. Proton NMR and EPR Spectroscopy of Paramagnetic Metalloporphyrins. In *The Porphyrin Handbook*; Kadish, K. M., Smith, K. M., Guilard, R., Eds.; Academic Press: San Diego, CA, 2000; Vol. 5, Chapter 36, pp 81−183.
(15) Walker, F. A. *Inorg. Chem.* **2003**, *42*, 4526−4544.
(16) La Mar, G. N.; Bold, T. J.; Satterlee, J. D. *Biochim. Biophys. Acta* **1977**, *498*, 189−207.
(17) Safo, M. K.; Nesset, M. J. M.; Walker, F. A.; Debrunner, P. G.; Scheidt, W. R. *J. Am. Chem. Soc.* **1997**, *119*, 9438−9448.
(18) Yatsunyk, L. A.; Carducci, M. D.; Walker, F. A. *J. Am. Chem. Soc.* **2003**, *125*, 15986−16005.
(19) Ikeue, T.; Saitoh, T.; Yamaguchi, T.; Ohgo, Y.; Nakamura, M.; Takahashi, M.; Takeda, M. *Chem. Commun.* **2000**, 1989−1990.
(20) Ikeue, T.; Ohgo, Y.; Yamaguchi, T.; Takahashi, M.; Takeda, M.; Nakamura, M. *Angew. Chem., Int. Ed.* **2001**, *40*, 2617−2620.
(21) Ohgo, Y.; Ikeue, T.; Nakamura, M. *Inorg. Chem.* **2002**, *41*, 1698−1700.
(22) Masuda, H.; Taga, T.; Osaki, K.; Sugimoto, H.; Yoshida, Z. I.; Ogoshi, H. *Inorg. Chem.* **1980**, *19*, 950−955.

S_4-saddled [FeOETPP(THF)$_2$]ClO_4 and S_4-ruffled [FeT^iPrP-(THF)$_2$]ClO_4, $S = {}^3/_2$ electronic states are observed, on the basis of NMR, EPR, Mössbauer, and magnetic data.[19] In ^{1}H NMR spectroscopic studies, the IS state exhibits fairly large downfield shifts of the pyrrole-β protons (or methylene protons in the case of the OETPP porphyrin core), indicating considerable π-symmetry spin density at the β-pyrrole carbons. In the EPR spectra, the signals around $g \sim 4$ and 2 are also consistent with the presence of the IS state. Further, the IS state is supported by the magnetic moment determined by liquid (Evans) and solid state (SQUID) methods. The latter resulted in an almost constant magnetic moment of 3.80 $\pm$ 0.09 μ_B and 3.90 $\pm$ 0.10 μ_B at 50−300 K for [FeOETPP(THF)$_2$]ClO_4[19] and [FeT^iPrP(THF)$_2$]ClO_4,[20] respectively. When a stronger-coordinating ligand is considered, namely, 4-CNPy, results interpreted as showing a novel spin crossover, LS ($S = {}^1/_2$) $\leftrightarrow$ IS ($S = {}^3/_2$), were observed for [FeOETPP(4-CNPy)$_2$]ClO_4,[20] and later for [FeOMTPP-(4-CNPy)$_2$]ClO_4 and a related octaalkyltetraphenylporphyrinate,[10] and a pure LS state with a $(d_{xz},d_{yz})^4(d_{xy})^1$ electron configuration for [FeT^iPrP(4-CNPy)$_2$]ClO_4, even though in all cases short Fe−N_p distances are expected.[19] Therefore, it appears that the binding ability of the axial ligand is an important factor in tuning the ground state of strongly distorted porphyrins. 4-CNPy is an interesting ligand, because when combined with various porphyrin cores it can result in LS or IS complexes.[5,6,10,20]

We have further investigated the NMR, EPR, and solution magnetic susceptibility of [FeOETPP(4-CNPy)$_2$]ClO_4 and related compounds with different S_4-saddled porphyrin cores, namely [FeOMTPP(4-CNPy)$_2$]ClO_4 and [FeTC_6TPP-(4-CNPy)$_2$]ClO_4, in order to gain a better understanding of the factors that influence the ground state and electronic properties of these complexes. Just at the time this paper was submitted, a paper was published in this journal that included NMR and EPR investigations of the same iron(III) porphyrinates.[10] Although some of the basic conclusions reached in these two studies are the same, others differ markedly, and some of the experimental results differ as well. The major focus of this research is the correlation of solution spectroscopic data with the structural parameters obtained from X-ray crystallography. In the course of these investigations, we have obtained evidence that [FeOETPP(4-CNPy)$_2$]-ClO_4 is not a pure IS complex, but rather a new electron configuration for iron porphyrinates is observed, an $S = 2$ Fe(II) center antiferromagnetically coupled to an $S = {}^1/_2$ porphyrin π-cation radical, yielding an overall $S = {}^3/_2$ complex that can only be differentiated from intermediate spin (IS) Fe(III) by careful analysis of the proton NMR shifts, while both EPR spectra and magnetic susceptibility measurements are indicative only of the overall spin, $S = {}^3/_2$. The kinetics of inversion of the saddled porphyrinate complexes have also been investigated by DNMR and/or NOESY/EXSY techniques. The conclusions reached, on the basis of detailed 1- and 2-dimensional ^{1}H NMR spectroscopy and careful analysis of the chemical shifts and their temperature dependence, thus differ markedly from those presented previously. Molecular structures have been used in the present work to help arrive at an understanding of the NMR results, and these serve to strengthen the case of the current presentation.

Experimental Section

Synthesis. (OETPP)FeCl, (OMTPP)FeCl, and (TC_6TPP)FeCl were synthesized by previously reported methods.[18] The conversion of (OMTPP)FeCl to (OMTPP)$FeClO_4$ was carried out by the procedure developed earlier in this laboratory:[25] 72 mg (0.088 mmol) of (OMTPP)FeCl was dissolved in a small amount of freshly distilled THF (~5 mL) and heated; before reflux started, 7.3 mL of 0.012 M solution of $AgClO_4$ in THF (0.088 mmol of $AgClO_4$) was added at one time. *Caution! Perchlorate salts are potentially explosive when heated or shocked. Handle them in milligram quantities with care.* The mixture was refluxed for 15 min, cooled to ambient temperature, and filtered using a fine or medium glass frit filter. An equal amount of freshly distilled toluene was added then, and solvents were removed under vacuum at 50 °C. The residue was dissolved in a small amount of boiling toluene, and an equal volume of boiling heptane was added. After 1 day, starlike crystals formed; they were filtered, washed with cold heptane, and dried under vacuum at 60 °C for 4 h. (OETPP)$FeClO_4$ and (TC_6TPP)$FeClO_4$ were prepared in a similar fashion. In all three cases, the crystalline material contained a large amount of toluene. Therefore, before NMR samples were prepared, the crystals were dissolved in CH_2Cl_2, the solvent was removed under reduced pressure, and the residue was kept under vacuum overnight in order to remove any traces of toluene.

(OETPP)$FeClO_4$. ^{1}H NMR (CD_2Cl_2, 23 °C, 300 MHz, δ, ppm) 13.0 (8H, *o*), 9.8 (4H, *p*), 7.2 (8H, *m*), 0.6 (24H, CH_3); the methylene protons are too broad to be detected at ambient temperatures but are expected in the downfield region.

(OMTPP)$FeClO_4$. ^{1}H NMR (CD_2Cl_2, 22 °C, 300 MHz, δ, ppm) 60.6 (24H, CH_3), 12.0 (8H, *o*), 9.44 (4H, *p*), 7.6 (8H, *m*).

(TC_6TPP)$FeClO_4$. ^{1}H NMR (CD_2Cl_2, 23 °C, 300 MHz, δ, ppm) 89.8 (16, $CH_2(\alpha)$), 11.4 (8H, *o*), 9.2 (4H, *p*), 7.7 (8H, *m*), 1.7 (16H, $CH_2(\beta)$). ESI: $[FeTC_6TPP]^+$ $m/z = 884$, $[^{35}ClO_4]^-$ $m/z = 99$, and $[^{37}ClO_4]^-$ $m/z = 101$. In all three samples, ClO_4^- is not bound (or weakly bound) to Fe(III); therefore, only one peak is observed for each phenyl-*ortho*, and -*meta* as well as CH_3 groups in OETPP and OMTPP and $CH_2(\beta)$ groups in TC_6TPP. Because elemental analysis was not carried out on these compounds, the solvent content of the crystalline solids is not known, although the heating to 60° in a vacuum for 4 h should in principle have removed solvent molecules.

[FeOETPP(4-CNPy)$_2$]ClO_4 samples were prepared by adding a solution of 5 mg (0.005 mmol) of (OETPP)$FeClO_4$ in 0.5 mL of CD_2Cl_2 to 1.6 mg (0.015 mmol) of 4-cyanopyridine in a 5 mm NMR tube to produce a complex concentration of 10 mM, with 10 mM free 4-CNPy if the complex is fully formed. The mixture was heated in a warm water bath for 5 min. There was no evident color change in the greenish-brown solution. Since no free (F) 4-CNPy peaks were observed in the proton NMR spectra at temperatures as low as −70 °C (203 K), another 0.0015 mmol of 4-CNPy was added. With this amount of axial ligand (total [4-CNPy] = 60 mM), free 4-CNPy peaks were observed below −30° (243 K), indicating

(23) Ogho, Y.; Saitoh, T.; Nakamura, M. *Acta Crystallogr., Sect. C* **1999**, *55*, 1284−1286.
(24) Chen, L.; Yi, G.-B.; Wang, L.-S.; Dharmwardana, U. R.; Dart, A. C.; Khan, M. A.; Richter-Addo, G. B. *Inorg. Chem.* **1998**, *37*, 4677−4688.
(25) Nesset, M. J. M., Ph.D. Dissertation, University of Arizona, 1994.

that ligand exchange (dissociation of coordinated ligand and binding of free 4-CNPy) is fast at higher temperatures. NMR data were acquired over 5° temperature intervals from 243 to 183 K, and at the end a greater than 10-fold excess of axial ligand was added and the ^{1}H 1D NMR experiments were repeated over the same temperature range. This was done in order to ensure that the amount of axial ligand in the sample was high enough for full complexation and that the chemical shifts and ligand exchange observed were due only to the specific binding properties of the 4-CNPy and not to its concentration. Chemical shifts, relaxation times, T_1, of all resonances, and the temperature at which free and bound 4-CNPy peaks appeared in the spectra were essentially the same with excess ligand.

In the same manner, [FeOMTPP(4-CNPy)$_2$]ClO$_4$ was prepared starting from (OMTPP)FeClO$_4$. The color of the complex changed from greenish-brown to cherry red upon addition of 4-CNPy. All ^{1}H 1D experiments were repeated 3 times with increasing ligand concentration: 29, 48, and 82 mM 4-CNPy. The chemical shift of the porphyrin CH$_3$ at 295 K changed from 65.9 to 62.6 ppm upon going from the lowest to highest ligand concentration. Chemical shifts of all other resonances also changed slightly. However, when the temperature was lowered below 213 K, all three samples showed very similar chemical shifts for all resonances. Finally, [TC$_6$TPP-(4-CNPy)$_2$]ClO$_4$ was prepared by dissolving 2 mg of (TC$_6$TPP)-FeClO$_4$ and 2 mg of 4-CNPy in 0.3 mL of CD$_2$Cl$_2$ to produce a sample having [TC$_6$TPPFeClO$_4$] = 6.7 mM and total [4-CNPy] = 21 mM. Free ligand peaks appeared below 213 K, indicating fast ligand exchange above this temperature. After NMR data were acquired, a 10-fold excess of axial ligand was added, and the ^{1}H 1D experiments were repeated. Relaxation times were measured again and showed no dependence upon axial ligand concentration for all peaks except for free 4-CNPy, for which T_1 increased, with increase in ligand concentration. In this case, the free ligand peaks appeared at 223 K and below. All the chemical shifts were the same for both samples at temperatures below 233 K.

On the basis of the differential effect of ligand concentration, the binding constants of 4-CNPy to the three iron(III) porphyrinates decrease in the order OETPP > TC$_6$TPP > OMTPP; however, no attempt was made to accurately measure the binding constants.

EPR spectra were recorded on a Bruker ESP-300E EPR spectrometer operating at 9.4 GHz, with 100 kHz field modulation and equipped with Oxford Instruments ESR 900 continuous flow helium cryostat. Spectra were obtained in frozen CD$_2$Cl$_2$ solutions and as crystalline samples at 4.2 K. Microwave frequencies were measured using a Systron-Donner frequency counter.

^{1}H NMR spectra were acquired using a Varian Unity-300 spectrometer operating at a ^{1}H 299.964 MHz and equipped with a broad-band inverse probe and variable-temperature unit. All spectra were recorded in CD$_2$Cl$_2$ in the temperature range 180−308 K and referenced to the residual solvent peak at 5.32 ppm. In the case of [FeOETPP(4-CNPy)$_2$]ClO$_4$, other solvents were used as well: CDCl$_3$ (δ_r = 7.24 ppm) in the temperature range from 303 to 330 K and C$_2$D$_2$Cl$_4$ (δ_r = 5.91 ppm) in the range from 303 to 363 K. One-dimensional spectra were collected using the standard one-pulse experiment with maximum spectral bandwidth of 40 kHz, a block size of 80 K data points, an approximate 90° pulse, and 100 transients. Homonuclear ^{1}H 2D spectra were acquired in States mode at a number of temperatures between 184 and 308 K using standard pulse sequences with 512 complex points in the directly detected dimension and 128 t_1 increments. The mixing time in NOESY/ROESY experiments was set to the average T_1 of the protons that are closest to the paramagnetic center (usually *ortho*-phenyl-H, the protons of coordinated 4-CNPy, the methylene protons in OETPP and TC$_6$TPP complexes, or methyl protons in the OMTPP complex). The relaxation delays in 2D experiments were set so that the total recycle time was longer or equal to the T_1 of the *para*-phenyl protons, which are typically the slowest relaxing protons of the complex, or to the average of the T_1's of the free ligand protons. NOESY/ROESY spectra were processed using the Felix 2000 software package (Molecular Simulations). Data were zero-filled to twice the original data size in both dimensions before applying Gaussian apodization. After Fourier transformation, baseline correction was done by detecting the baseline points using the FLATT procedure,[26] and fitting the points to an *n*th-order polynomial (*n* can vary from 1 to 5). COSY and DQF-COSY data were processed using standard VNMR software. Zero-filling and unshifted sine bell apodization functions were applied before each of the two Fourier transforms followed by baseline.

Solution magnetic susceptibilities were determined as a function of temperature by the method of Evans[27,28] in the range from 308 to 180 K with 5 K increments in specially constructed Wilmad coaxial tubes. Measurements were carried out on 10−14 mM porphyrin solutions in CD$_2$Cl$_2$ that contained approximately 1% of Me$_4$Si and 150−250 mM 4-CNPy and the same concentration of Me$_4$Si and 4-CNPy in the reference (outer) tube. The molar magnetic susceptibility, χ_M, for a long cylindrical sample oriented parallel to the magnetic field, **B**, is calculated according to the following equation[28]

$$\chi_M = \frac{\chi_0 \cdot \mathrm{MW(solute)}}{\mathrm{MW(solvent)}} + 3000\frac{\Delta\nu}{4\pi \cdot \nu_0 \cdot C} \qquad (1)$$

where χ_0 is the diamagnetic molar susceptibility of the pure solvent (-46.6×10^{-6} for CD$_2$Cl$_2$), ν_0 is the spectrometer frequency in Hz; $\Delta\nu$ is the difference in chemical shifts between the Me$_4$Si signals in the inner and outer tubes of the sample, in Hz; C is the concentration of porphyrin in mol/L. The value of χ_M thus obtained is then corrected for diamagnetic contributions from the porphyrin anion, axial ligands, and iron using Pascal's constants,[29,30] and finally, the effective magnetic moment, μ_{eff}, is calculated according to

$$\mu_{eff} = 2.84\sqrt{\chi_M' T} \qquad (2)$$

where χ_M' is the corrected molar susceptibility. The accuracy of the results obtained depends on the accurate knowledge of concentration and the accurate determination of $\Delta\nu$ and is never better than 5%. Because it is possible that at least one solvent molecule (CH$_2$Cl$_2$) was present in the crystals of each of the iron porphyrinate complexes of this study, the concentrations of the complexes could be 9−10% (for one) or 18−20% (for two molecules of CH$_2$Cl$_2$) less than expected on the basis of the formula weight of the compounds themselves, meaning that the magnetic moments of the complexes are likely on the order of 5−10% larger than shown in Figure 5. The total diamagnetic corrections for [FeOETPP(4-CNPy)$_2$]$^+$, [FeOMTPP(4-CNPy)$_2$]$^+$, and [FeTC$_6$TPP-(4-CNPy)$_2$]$^+$ are -618.3×10^{-6}, -523.4×10^{-6}, and -591.7×10^{-6}, respectively.

Porphyrin ring inversion in [FeOETPP(4-CNPy)$_2$]ClO$_4$ is an example of a symmetrical two-site exchange with equal population

(26) Güntert, P.; Wüthrich, K. *J. Magn. Reson.* **1992**, *96*, 403−407.
(27) Evans, D. F. *J. Chem. Soc.* **1959**, 2003−2005.
(28) Sur, S. K. *J. Magn. Reson.* **1989**, *82*, 169−173.
(29) Mabbs, F. E.; Machin, D. J. *Magnetism and Transition Metal Complexes*; Chapman and Hall: London, 1973.
(30) Kahn, O. *Molecular Magnetism*; VCH: New York, 1993.

of the two forms.[31] It was studied using NOESY/EXSY experiments in the temperature range from 243 to 308 K in CH_2Cl_2 and from 313 to 333 K in $CDCl_3$. Mixing times, τ_m's, were set on the order of the T_1 of the methylene protons, namely from 3 to 10 ms, depending on temperature. The rate constants were calculated using the following equation

$$k_{ex} = \frac{I_{diag}}{(I_{cross} + I_{diag}) \times \tau_m} \quad (3)$$

where I_{diag} and I_{cross} are the intensities (volumes) of the diagonal and cross-peaks, respectively, and τ_m is the mixing time used in the NOESY experiment.[31,32] The volumes of the diagonal and cross-peaks, measured using Varian VNMR software, were averaged before being used for calculations. All experiments were done 2−3 times at a given temperature with different mixing times to obtain higher accuracy.

Porphyrin Ring Inversion in [FeTC$_6$TPP(4-CNPy)$_2$]ClO$_4$. For two-site chemical exchange that is fast on the NMR time scale (above the coalescence temperature, T_c, where only the averaged chemical environment of two exchanging species can be detected), the modified Bloch equations can be simplified to the expression[31]

$$k_{ex} = \frac{\pi(\Delta\nu)^2}{2(W^* - W_0)} \quad (4)$$

where $\Delta\nu$ is the difference in the chemical shift (in Hz) between two exchanging species extrapolated to temperatures above T_c, W^* is the width at half-height of the exchange-broadened line, and W_0 is the inherent line width at half-height (usually it is measured at high temperatures where chemical exchange is extremely fast on the NMR time scale or at very low temperatures in the absence of chemical exchange). The difference in the denominator indicates how much the NMR line was broadened due to the presence of chemical exchange only, eliminating the influence of NMR parameters such as line broadening due to increased solvent viscosity, miscalibration of the pulses, truncation of FIDs, and others. In the case of diamagnetic molecules, all values in eq 4, except W^*, remain constant with temperature. However, for paramagnetic molecules not only W^* but also W_0 and $\Delta\nu$ change with temperature, and all these changes should be taken into account.

The rate constants thus obtained were used for the determination of the activation parameters, $\Delta H^{\ddagger}$ and $\Delta S^{\ddagger}$, of ring inversion. The dependencies of $\ln(k_{ex}h/k_BT)$ on inverse temperature were plotted in Origin, and least squares linear regression fitting was applied. The slope and intercept of the linear fit were assigned to $\Delta H^{\ddagger}$ and $\Delta S^{\ddagger}$, respectively, according to the Eyring equation

$$\ln\frac{k_{ex}h}{k_BT} = -\frac{\Delta H^{\ddagger}}{RT} + \frac{\Delta S^{\ddagger}}{R} \quad (5)$$

where h is Planck's constant, k_B is Boltzmann's constant, T is temperature (K), and R is the gas constant.

Structure Determination. General. Crystals were grown by liquid diffusion methods. In all cases two solvent systems were used: (1) methylene chloride and dodecane; (2) chloroform and cyclohexane. Crystals of each complex were mounted on glass fibers in random orientation and examined on a Bruker SMART 1000 CCD detector X-ray diffractometer at 170(2) K. All measurements utilized graphite monochromated Mo Kα radiation (λ = 0.71073 Å) with a power setting of 50 kV and 40 mA. Final cell constants and complete details of the intensity collection and least squares refinement parameters for all complexes are summarized in Table 1.

In two cases, a total of 3736 frames at 1 detector setting covering $0° < 2\theta < 60°$ were collected, having an ω scan width of 0.2° and an exposure time of 20 s per frame. In the case of [FeOETPP-(4-CNPy)$_2$]ClO$_4$ from methylene chloride/cyclohexane, a total of 7372 frames at two detector settings with $2\theta = -17.50$ and $-33.5°$, covering $0° < 2\theta < 51°$, were collected having an ω scan width of 0.2° and an exposure time of 20 s per frame. The frames were integrated using the Bruker SAINT software package's narrow frame algorithm.[33] Initial cell constants and an orientation matrix for integration were determined from reflections obtained in three orthogonal 5° wedges of reciprocal space.

All structures were solved using SHELXS in the Bruker SHELXTL (Version 6.0) software package.[34] Refinements were performed using SHELXL, and illustrations were made using XP.[34] Solution was achieved utilizing direct (or in some cases Patterson) methods followed by Fourier synthesis. Hydrogen atoms were added at idealized positions, constrained to ride on the atom to which they are bonded and given thermal parameters equal to 1.2 or 1.5 times U_{iso} of that bonded atom. Although solvents of crystallization were deuterated, they were refined as $CHCl_3$ and CH_2Cl_2 and are thus listed as such in Table 1. Empirical absorption and decay corrections were applied using the program SADABS.[35] Scattering factors and anomalous dispersion were taken from International Tables (Vol C, Tables 4.2.6.8 and 6.1.1.4.). The details of the individual structure determinations are provided in the Supporting Information.

Results

[FeOMTPP(4-CNPy)$_2$]ClO$_4$ was obtained in one crystalline form from the $CDCl_3$/cyclohexane solvent system. [FeOETPP(4-CNPy)$_2$]ClO$_4$ was obtained in two different crystalline forms, from CD_2Cl_2/dodecane and $CDCl_3$/cyclohexane. We were not successful in obtaining the crystal structure of [FeTC$_6$TPP(4-CNPy)$_2$]ClO$_4$: two attempts at growing crystals of this complex resulted in two structures of 5-coordinate (TC$_6$TPP)Fe$^+$ with ClO_4^- and NO_3^- as axial ligands. These structures are not discussed here. Atomic coordinates, a table of complete bond length and angles, anisotropic thermal parameters, and hydrogen coordinates and complete torsion angles for all complexes in this study are listed in Tables S1−S15 in the Supporting Information.

Molecular Structure of [FeOMTPP(4-CNPy)$_2$]ClO$_4$. The molecular structure of [FeOMTPP(4-CNPy)$_2$]ClO$_4$ is displayed in Figure 1 together with the numbering scheme for the crystallographically unique atoms. The porphyrin is nonplanar and adopts a predominantly saddled conformation with some ruffling admixture. This conclusion was drawn upon close examination of the formal diagram and the linear

(31) Ernst, R. R.; Bodenhausen, G.; Wokaun, A. *Principles of Nuclear Magnetic Resonance in One and Two Dimensions*; Clarendon Press: Oxford, U.K., 1992; Chapter 9.
(32) Shokhirev, N. V.; Shokhireva, T. Kh.; Polam, J. R.; Watson, C. T.; Raffii, K.; Simonis, U.; Walker, F. A. *J. Phys. Chem. A* **1997**, *101*, 2778−2786.
(33) *SAINT Reference Manual Version 6.0*; Bruker AXS Inc.: Madison, WI, 2002.
(34) *SHELXTL Reference Manual Version 6.0*; Bruker AXS Inc.: Madison, WI, 2002.
(35) Sheldrick, G. M. *SADABS*, version 2.3; Universität Göttingen: Göttingen, Germany, 2002.

Table 1. Experimental Details Together with Crystal Data for [FeOMTPP(4-CNPy)$_2$]ClO$_4$, and [FeOETPP(4-CNPy)$_2$]ClO$_4$

	[FeOMTPP(4-CNPy)$_2$]-ClO$_4$·CHCl$_3$	[FeOETPP(4-CNPy)$_2$]-ClO$_4$·1.5CH$_2$Cl$_2$	[FeOETPP(4-CNPy)$_2$]-ClO$_4$·2CHCl$_3$
empirical formula	$FeN_8C_{65}H_{53}O_4Cl_4$	$FeN_8C_{73.5}H_{71}O_4Cl_4$	$FeN_8C_{74}H_{70}O_4Cl_7$
fw	1207.80	1328.03	1439.38
T, K	170(2)	170(2)	170(2) K
wavelength, Å	0.71073	0.71073	0.71073 Å
cryst syst	monoclinic	monoclinic	triclinic
space group	$P2_1/n$	$P2_1$	$P\bar{1}$
a, Å	14.7529(16)	13.5691(10)	14.3386(4)
b, Å	23.115(3)	42.461(3)	21.7212(5)
c, Å	17.3580(19)	24.0093(18)	24.1113(6)
α, β, γ, deg	90, 98.505(3), 90	90, 100.699(2), 90	101.250(1), 99.050(1), 97.391(1)
V, Å^3	5854.2(11)	13592.6(17)	7174.4(3)
Z	4	8	4
D (calcd), g/cm^3	1.370	1.298	1.333
abs coeff., mm^{-1}	0.497	0.434	0.525
F(000)	2500	5552	2988
cryst dimensions, mm^3	0.33 × 0.25 × 0.15	0.37 × 0.30 × 0.20	0.27 × 0.20 × 0.17
θ limits	1.48−27.03°	1.29−22.01°	1.15−23.50°.
limiting indices	$-18 \le h \le 18$	$-14 \le h \le 14$	$-16 \le h \le 16$
	$-29 \le k \le 29$	$-44 \le k \le 44$	$-24 \le k \le 24$
	$-22 \le l \le 22$	$-25 \le l \le 25$	$-27 \le l \le 27$
reflns utilized	68928	106355	103862
indep reflns	12736 [$R_{int} = 0.0925$]	33209 [$R_{int} = 0.1154$]	103862 [$R_{int} = 0.0000$]
completeness	99.6%	99.54%	98.3%
abs corr	SADABS	SADABS	TWINABS
max and min transm	0.9292 and 0.8532	0.9182 and 0.8558	0.9160 and 0.8712
data/restraints/params	12736/12/773	33209/355/3350	103862/2270/1750
GOF on F^2	1.007	1.026	0.650
final *R* indices	R1 = 0.0555	R1 = 0.0707	R1 = 0.0660
[$I > 2\sigma(I)$]	wR2 = 0.1207	wR2 = 0.1675	wR2 = 0.0956
R indices (all data)	R1 = 0.1142	R1 = 0.1452	R1 = 0.2480
	wR2 = 0.1458	wR2 = 0.2106	wR2 = 0.1519
largest diff peak and hole	0.562; −0.426 e/Å^3	0.973; −0.583 e/Å^3	0.690; −0.608 e/Å^3
RMS difference density	0.071 e/Å^3	0.078 e/Å^3	0.101 e/Å^3

deviation of the porphyrinato core (Figure 2). The average deviations for adjacent β-carbons from the 24-atom mean plane are ±1.16 and ±0.96 Å, indicating some twisting of the pyrrole rings, consistent with a small ruffling component in the molecular structure. This is supported by the deviation of the *meso*-carbons, which are above and below the porphyrin mean plane by ±0.24 Å. The dihedral angle, $\Delta\varphi$, between the axial ligand planes is 64.3(1)°. However, it should be taken into account that one ligand is severely tilted by 24.4° with respect to the normal to the porphyrin plane, and this interferes with measurements of $\Delta\varphi$. This is, probably, one of the largest deviations of axial ligands from the porphyrin normal observed in bis(pyridine or imidazole) iron(III) porphyrinate complexes, and it appears to be due to crystal packing forces. In contrast, the tilt of the other ligand is only 1.6°. The dihedral angles φ between the axial ligand plane and the plane defined by the closest N_P-Fe-N_P vector and N5 and N7 (nitrogens coordinated to Fe) of the axial ligands are 10.4(1)° and 35.4(1)° for the two ligands, respectively, or −10.4(1)° and +54.6(1)° angles from the same N_P-Fe-N_P vector. While the first angle is typical for saddled porphyrins with perpendicular orientation of axial pyridine ligands, the second angle shows substantial deviation and is more typical of ruffled structures. The dihedral angles between the phenyl ring planes and the porphyrin mean plane are 44.6°, 53.7°, 44.2°, and 49.53°. In saddled porphyrins the phenyl rings are rotated toward the porphyrin mean plane in order to avoid steric interactions with the β-pyrrole substituents. Therefore, the value of the dihedral angle between the phenyl ring planes and porphyrin mean plane can be used as indication of the degree of saddled distortion; the smaller the dihedral angle between the phenyl planes and the porphyrin mean plane the greater the saddled distortion. The high degree of saddled conformation is associated with the large dihedral angles between a pair of the adjacent pyrrole rings (38.6°) and between a pair of opposite pyrrole rings (56.5°). However, these are smaller than the same angles for either of the [FeOETPP(4-CNPy)$_2$]ClO$_4$ structures discussed below.

The average values for chemically equivalent bond distances and angles with estimated standard deviations are shown in Figure 2. The average $Fe-N_P$ distance is 1.973(2) Å, and two $Fe-N_{ax}$ distances are 2.215(3) and 2.282(3) Å. The short $Fe-N_P$ distance is an indication of the strong nonplanar distortion of the porphyrin core, and the long $Fe-N_{ax}$ distance is consistent with the overall $S = {}^3/_2$ state of the complex (consisting of some degree of $S = 2$ Fe(II) and the same degree of $S = {}^1/_2$ porphyrin radical, antiferromagnetically coupled) observed in solution for [FeOMTPP(4-CNPy)$_2$]ClO$_4$ (see below).

Molecular Structure of [FeOETPP(4-CNPy)$_2$]ClO$_4$ from Methylene Chloride/Dodecane. There are 4 unique molecules in the asymmetric unit of [FeOETPP(4-CNPy)$_2$]ClO$_4$. The molecular structure of **1** is shown as an ORTEP diagram (Figure 3) along with the numbering scheme for the crystallographically unique atoms; all other porphyrins have similar basic features. The numbering schemes start with 2, 3, and 4 for porphyrins **2**, **3**, and **4**, respectively. The

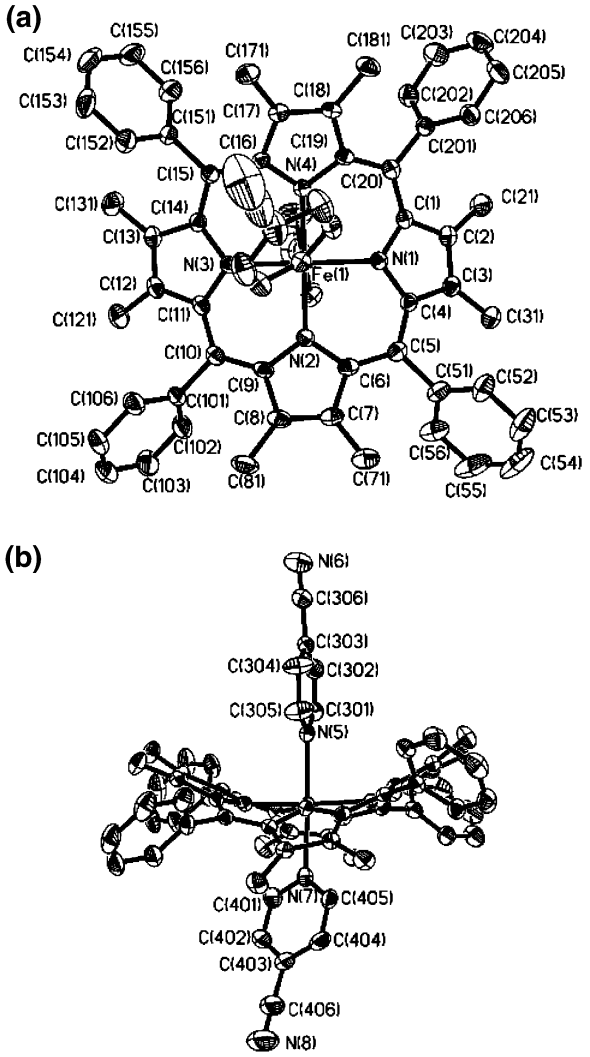

Figure 1. (a) ORTEP diagram of the porphyrin macrocycle of [FeOMTPP-(4-CNPy)$_2$]ClO$_4$ with the numbering scheme for the unique atoms: top view. Strong tilting of one of the axial ligands can be seen. (b) ORTEP plot of [FeOMTPP(4-CNPy)$_2$]ClO$_4$ showing arrangement and numbering scheme for axial ligands: edge-on view. Porphyrin core geometry is saddled with a substantial (17%) degree of ruffling reflected in the twisting of pyrrole rings. Thermal ellipsoids are shown at 50% probability. Hydrogen atoms have been omitted for clarity.

deviation of core atoms from the 25-atom mean porphyrin plane for all four molecules is displayed in Figure 4, together with the axial ligand orientations. The linear representation of the same deviations is shown in Figure S1A of the Supporting Information. All four molecules adopt a predominantly saddled conformation, with alternating pyrrole rings pointing up and down and *meso*-C's being close to or in the porphyrin mean plane. There are some important differences in the molecular structures of the four porphyrin molecules. Molecule **2** is purely saddled with an average deviation of the *meso*-C's from the porphyrin mean plane of 0.015 Å (see Table 2), while for all other complexes the average deviations of the *meso*-C's are more substantial: 0.078(9), 0.225(11), and 0.103(11) Å for **1**, **3**, and **4**, respectively. One can see that molecule **3** has the highest ruffling component of all four molecules. Normal-coordinate structural decomposition, NSD, calculations were carried out[36,37] using the core coordinates of the four porphyrin

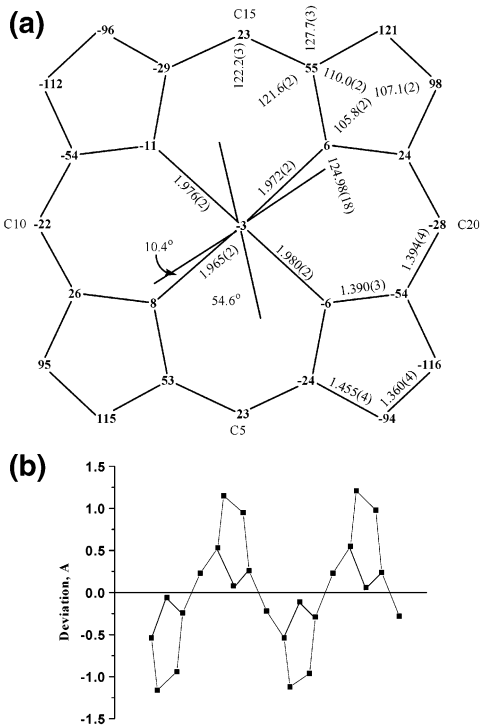

Figure 2. (a) Formal diagram of [FeOMTPP(4-CNPy)$_2$]ClO$_4$, showing the displacement of the atoms in units of 0.01 Å, from the mean plane of the 24-atom core. The orientations of the axial ligands with the closest Fe−N$_p$ vector and selected bond lengths and angles are also shown. The numbers given in parentheses are the estimated standard deviations. (b) Linear representation of the deviation of the macrocycle atoms from the mean porphyrin plane.

molecules in [FeOETPP(4-CNPy)$_2$]ClO$_4$, and the results are displayed in Table 3. According to the NSD method, the nonplanarity of the porphyrin core can be described in terms of displacements along the lowest-frequency normal coordinates of the porphyrin macrocycle in order to quantify the contribution from different types of distortion (saddled, ruffled, etc.). There are six out-of-plane displacements along the lowest frequency vibrational modes of the porphyrin core: B_{2u}(saddle), B_{1u}(ruffle), A_{2u}(dome), $E_g(x)$ (wave(x)), $E_g(y)$ (wave(y)), and A_{1u}(propeller).[36,37] As seen from the results in Table 3, all molecules display predominantly saddled conformations with large B_{2u} parameter. The B_{1u} parameter (ruffling) is small for all molecules except **3**, where it is equal to 0.6489. This results in a 14% ruffling component in the otherwise saddled structure of **3**. The ruffling contribution is still not as high as in the structure of [FeOMTPP-(4-CNPy)$_2$]ClO$_4$, where it is equal to 17%. The contributions from the other types of nonplanar distortion are either small or absent.

In molecules **3** and **4**, the axial ligands are in close to perpendicular planes (see Figure 4), with actual dihedral angles, $\Delta\varphi$, of 84.2° and 87.3°, respectively. But molecules **1** and **2** have substantially smaller dihedral angles of 79.4° and 67.1°. The latter is one of the smallest angles observed for saddled iron porphyrinates with planar aromatic ligands,

(36) (a) Jentzen, W.; Ma, J.-G.; Shelnutt, J. A. *Biophys. J.* **1998**, *74*, 753−763. (b) Jentzen, W.; Song, X.-Z.; Shelnutt, J. A. *J. Phys. Chem. B* **1997**, *101*, 1684−1699.
(37) http://jasheln.unm.edu/jasheln/content/nsd/NSDengine.

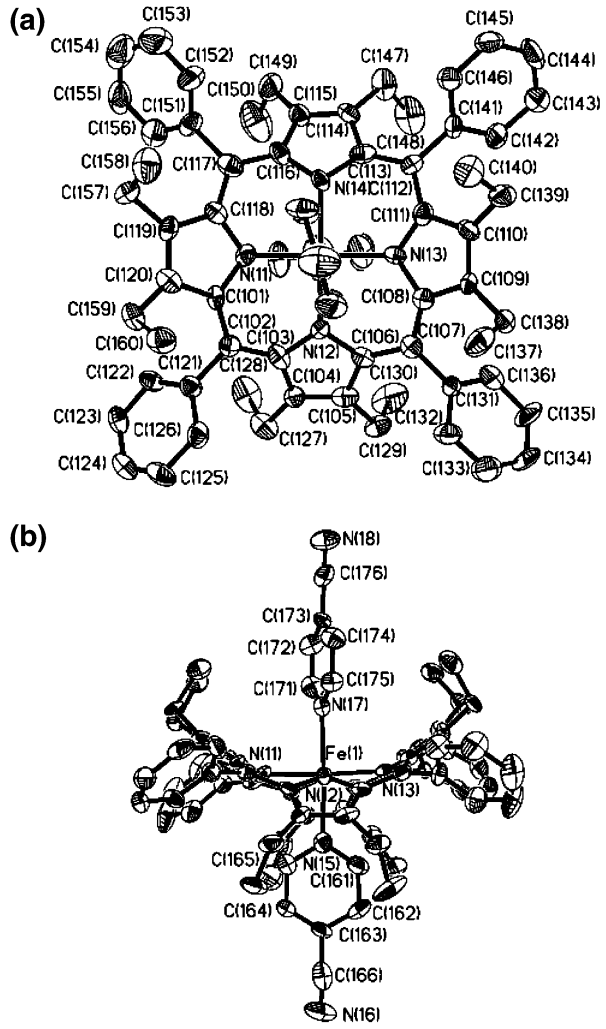

Figure 3. (a) ORTEP diagram of porphyrin macrocycle in [FeOETPP-(4-CNPy)$_2$]ClO$_4$: top view. Only porphyrin molecule **1** is shown. All the other porphyrins have similar molecular structures and numbering schemes except that all numbers start with 2, 3, and 4 for porphyrins **2**, **3**, and **4**, respectively. (b) ORTEP diagram of the porphyrin **1** together with the numbering scheme for the axial ligands: edge-on view. The porphyrin core in **1** adopts close to ideal saddled geometry. Thermal ellipsoids enclose 50% probability, and hydrogens are omitted for clarity.

with the notable exception of *paral*-[FeOMTPP(1-MeIm)$_2$]$^+$, in which the ligand plane dihedral angle is 19.5°.[18] In all four molecules, **1**−**4**, the axial ligand planes are fairly close to eclipsing the N$_P$−Fe−N$_P$ axis. The φ angles are 16° and 5° in **1**, 10° and 15° in **2**, 22° and 22° in **3**, and 16° and 15° in **4**. Only in the case of **3** are the angles between the N$_P$−Fe−N$_P$ axis and the projection of the axial ligands onto the porphyrin mean plane somewhat large. This larger angle contributes to the fact that the molecular structure of **3** has a substantial degree of ruffling. In comparison, [FeTMP(4-CNPy)$_2$]ClO$_4$[5] and [FeTPP(4-CNPy)$_2$]ClO$_4$[6] complexes adopt a ruffled geometry, are much less distorted from planarity, and have axial ligands in close to perpendicular planes located over the *meso* carbons. This also holds true for Fe(III)TMP structures with other weakly basic pyridines such as 3-ClPy.[5]

The 4-CNPy ligands in **1** and **2** are nearly perpendicular to the porphyrin core with the dihedral angles between the ligand planes and porphyrin mean plane equal to 88.8° and 87.8° in **1**, and 84.0° and 83.0° in **2**. But in the molecular structure of **3** and **4**, substantial deviation occurs: the corresponding dihedral angles are 84.2° and 74.0° in **3** and 87.0° and 78.5° in **4**. Similar values to those in **3** are observed in [FeTMP(4-CNPy)$_2$]ClO$_4$.[5]

The average dihedral angles between the porphyrinato core and the phenyl rings are relatively small, 40.1°, 40.6°, 41.1°, and 42.2° in **1**, **2**, **3**, and **4**, respectively, and indicate a high degree of saddled distortion. For ruffled [FeTPP(4-CNPy)$_2$]-ClO$_4$, these angles are much higher, with the average value being 61.8°.[6] The other evidence of the highly saddled distortion in **1**−**4** is the angle between adjacent and opposite pyrrole rings. The saddled conformation is associated with a large dihedral angle between the opposite pyrrole rings. Angles of 67.0°, 66.0°, 68.1°, and 66.1° are observed for **1**, **2**, **3**, and **4**, respectively. Angles between adjacent pyrrole rings are also large: 46.0°, 44.8°, 46.9°, and 45.0° for **1**, **2**, **3**, and **4**, respectively.

The average values for selected bond distances and angles with estimated standard deviation for **1**−**4** as well as for **5**−**6** ([FeOETPP(4-CNPy)$_2$]ClO$_4$ from CDCl$_3$/cyclohexane) are included in Figure 4. Average Fe−N$_P$ distances are relatively short: 1.966(8), 1.967(8), 1.961(8), and 1.958(8) Å for **1**, **2**, **3**, and **4**, respectively, indicating a large deformation of the porphyrin core. In contrast, the Fe−N$_{ax}$ distances are long, 2.191(9) and 2.199(9), 2.167(9) and 2.214(11), 2.228(8) and 2.240(9), and 2.175(9) and 2.214(10) Å for **1**, **2**, **3**, and **4**, respectively. These distances correlate well with the same distances in [FeOMTPP(4-CNPy)$_2$]ClO$_4$, **5** and **6**, and are typical for $S = {}^3/_2$ porphyrinatoiron(III) complexes.

Molecular Structure of [FeOETPP(4-CNPy)$_2$]ClO$_4$ from Chloroform/Cyclohexane. There are two independent molecules, **5** and **6**, on general positions in the asymmetric unit. The molecular structure of **5** is displayed in the ORTEP diagram, Figure S2, together with the numbering scheme for crystallographically unique atoms. The relative orientation of the axial 4-CNPy ligands is close to perpendicular, as observed in molecules **1**−**4** of the other [FeOETPP(4-CNPy)$_2$]$^+$ crystalline form. One of the eight ethyl groups points in the direction opposite from expected, suggesting a low barrier for ethyl group rotation. Apart from that, structures **5** and **6** share all the basic features of structures **1**−**4**. Average values for the chemically equivalent bond distances and angles, deviations of the core atoms from the porphyrin mean plane, and the orientation of the axial pyridine ligands are shown in the formal diagram (Figure 4). From Figure 4 and also from the linear display of the core atom deviations (Figure S1B), one can see that both **5** and **6** adopt close to purely saddled conformation with a small ruffling admixture, which is reflected in the slight twisting of the pyrrole rings and in the deviation of the *meso*-carbons from the mean plane (0.233(5) and 0.088(5) Å for **5** and **6**, respectively). However, **5** is more distorted from purely saddled geometry than **6**. Adjacent pyrrole β-carbons are above and below the porphyrin mean plane by ±1.156-(5), ±1.337(5) Å, and ±1.183(5), ±1.257(5) Å with differences of 0.181 Å and 0.074 Å for **5** and **6**, respectively. NSD calculations[37] (see Table 3) showed that **5** is overall

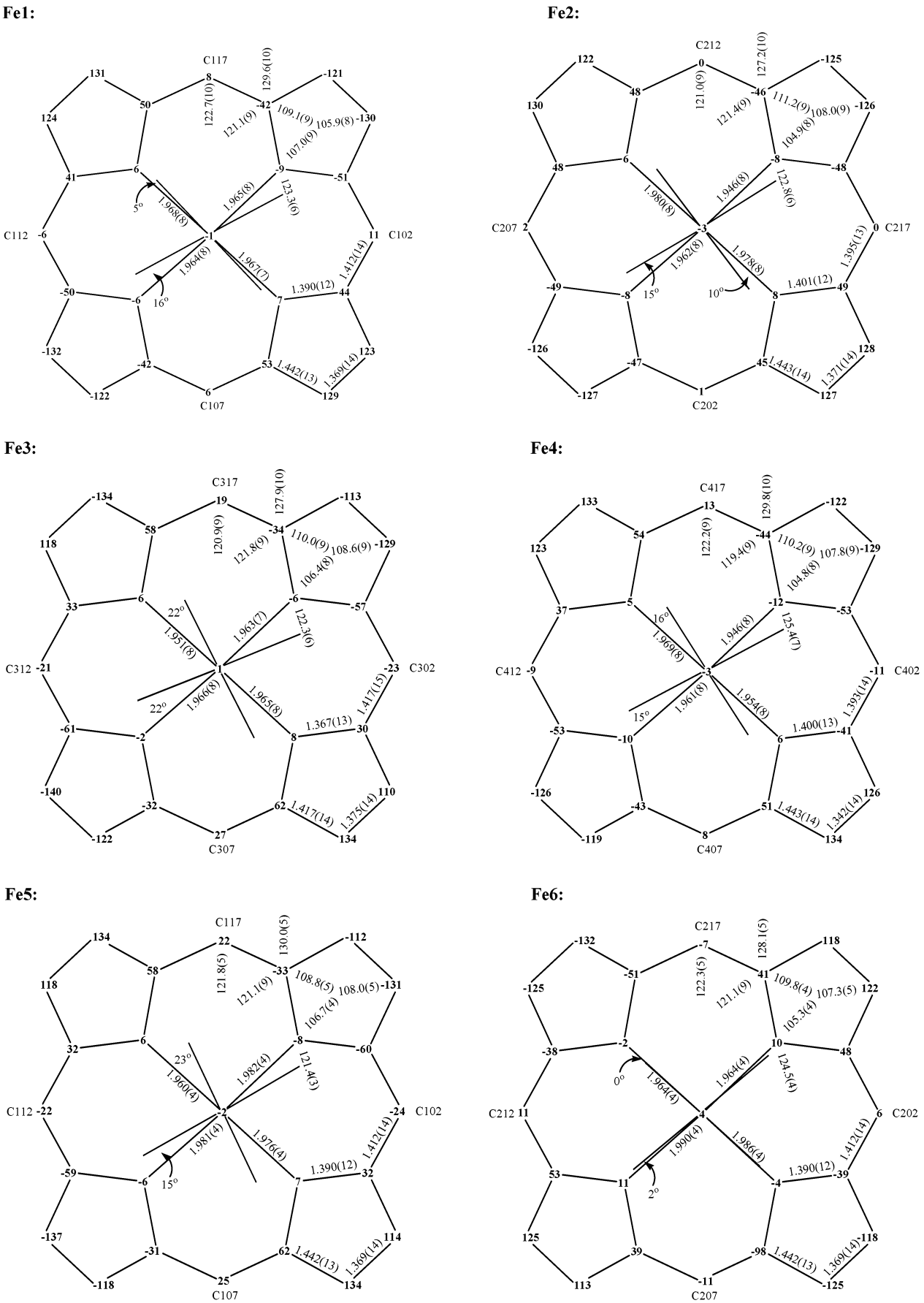

Figure 4. Formal diagram of $[FeOETPP(4\text{-}CNPy)_2]ClO_4$ molecules **1**−**6** showing the displacement of the atoms, in units of 0.01 Å, from the mean plane of the 25-atom core of each. The orientations of the axial ligands with the closest N_P-Fe−N_P vector and selected bond lengths and angles are also shown.

Table 2. Comparison of Structural Parameters for Complexes in This Study

compd	Fe−N_P, Å	Fe−N_{ax}, Å	av $\|\Delta C_m\|$, Å	av $\|\Delta C_\beta\|$, Å	angle φ between N−Fe−N axis and ligand planes, deg	dihedral angle, $\Delta\varphi$, deg	av dihedral angles of phenyls, deg
$[FeOMTPP(4\text{-}CNPy)_2]ClO_4\cdot CHCl_3$	1.973(2)	2.215(2) 2.282(3)	±0.240	±1.16; ±0.96	−10.4; 54.6	64.3(1)	48.0
$[FeOETPP(4\text{-}CNPy)_2]ClO_4\cdot CH_2Cl_2$, **1**	1.966(8)	2.191(9) 2.199(9)	±0.078	±1.23; ±1.31	−5.4; 74.0	79.4(4)	40.1
$[FeOETPP(4\text{-}CNPy)_2]ClO_4\cdot CH_2Cl_2$, **2**	1.967(8)	2.167(9) 2.214(11)	±0.015	±1.25; ±1.27	+15.2; 79.9	67.1(4)	40.6
$[FeOETPP(4\text{-}CNPy)_2]ClO_4\cdot CH_2Cl_2$, **3**	1.961(8)	2.228(8) 2.240(9)	±0.225	±1.16; ±1.34	−22.0; 67.6	84.2(3)	41.1
$[FeOETPP(4\text{-}CNPy)_2]ClO_4\cdot CH_2Cl_2$, **4**	1.958(8)	2.175(9) 2.214(10)	±0.103	±1.23; ±1.30	−15.6; 75.5	87.3(5)	42.2
$[FeOETPP(4\text{-}CNPy)_2]ClO_4\cdot CHCl_3$, **5**	1. 975(4)	2.203(4) 2.269(5)	±0.233	±1.16; ±1.34	−14.5; 67.4	78.6(2)	42.9
$[FeOETPP(4\text{-}CNPy)_2]ClO_4\cdot CHCl_3$, **6**	1.976(4)	2.262(4) 2.267(5)	±0.088	±1.18; ±1.26	+1.7; 89.9	88.2(2)	42.2

Table 3. Normal-Coordinate Structural Decomposition (NSD)[36,37] of Distortion Modes of the Complexes of This Study

compd	B_{2u}, saddle	B_{1u}, ruffle	A_{2u}, dome	$E_g(x)$, wave(x)	$E_g(y)$, wave(y)	A_{1u}, propeller	sum	av $\|\Delta C_m\|$, Å	av $\|\Delta C_\beta\|$, Å	ruf/sum %
$[FeOMTPP(4\text{-}CNPy)_2]ClO_4\cdot CHCl_3$	3.2044	0.6815	0.0442	0.0580	0.0683	0.0206	4.077	±0.24	±1.16; ±0.96	17.0
$[FeOETPP(4\text{-}CNPy)_2]ClO_4\cdot CH_2Cl_2$, **1**	3.8142	0.2236	0.0299	0.0355	0.0440	0.0218	4.1690	±0.078	±1.23; ±1.31	5.0
$[FeOETPP(4\text{-}CNPy)_2]ClO_4\cdot CH_2Cl_2$, **2**	3.8141	0.0296	0.0180	0.0251	0.0431	0.0338	3.9637	±0.15	±1.25; ±1.27	0.7
$[FeOETPP(4\text{-}CNPy)_2]ClO_4\cdot CH_2Cl_2$, **3**	3.7623	0.6489	0.0425	0.1324	0.0632	0.0276	4.6769	±0.225	±1.16; ±1.34	14.0
$[FeOETPP(4\text{-}CNPy)_2]ClO_4\cdot CH_2Cl_2$, **4**	3.8204	0.2806	0.1003	0.0551	0.0410	0.0226	4.3200	±0.103	±1.23; ±1.30	6.5
$[FeOETPP(4\text{-}CNPy)_2]ClO_4\cdot CHCl_3$, **5**	3.7632	0.6603	0.0045	0.0706	0.0211	0.0066	4.5263	±0.233	±1.16; ±1.34	14.6
$[FeOETPP(4\text{-}CNPy)_2]ClO_4\cdot CHCl_3$, **6**	3.6813	0.2555	0.1079	0.0266	0.0929	0.0084	4.1726	±0.088	±1.18; ±1.26	6.0

somewhat more distorted from planarity (the sum of all vibrational coefficients, 4.5263, is larger than the corresponding sum for complex **6**, 4.1726) and has a higher degree of ruffled distortion: 15% for **5** versus 6% for **6**.

Axial ligand plane orientations in both **5** and **6** are close to perpendicular. In **5**, the dihedral angle between axial ligand planes, $\Delta\varphi$, is 78.6(2)°, forming 14.5(2)° and 22.7(2)° angles to the closest N_P−Fe−N_P vector for ligand 1, L1 (N15), and ligand 2, L2 (N17), respectively. Similar values are observed for the structure of **6**, which has $\Delta\varphi$ of 88.2(2)°. In this case, the ligands are only 1.7(2)° and 0.1(2)° away from the closest N_P−Fe−N_P bond for L1 (N25) and L2 (N27), respectively. These, together with the small tilt of the axial ligands (89.7(1)° and 85.7(2)° for L1 and L2, respectively), create a very symmetrical environment for the Fe atom in **6**. In **5**, the axial ligands are more tilted with respect to the porphyrin mean plane, forming 82.3(1)° and 78.3(1)° dihedral angles for L1 and L2, respectively.

The observed average dihedral angles of the phenyls are 42.9° and 42.2° for **5** and **6**, respectively. The acute dihedral angles of phenyls are an indication of a severe saddled distortion of the porphyrin core. The average C_{Porph}−C_{Ph} distances are 1.483(7) and 1.485(7) Å for **5** and **6**, respectively.

The average dihedral angle between the planes of adjacent pyrrole rings and the average dihedral angle between the opposite pyrrole rings are higher for **5** as compared to **6** (47.06° vs 43.67° for adjacent and 68.03° and 64.45°, for opposite) reflecting a higher degree of saddle distortion in **5**. In fact, **6** has the smallest saddled distortion compared to all other structures of $[FeOETPP(4\text{-}CNPy)_2]^+$.

The average Fe−N_P bond distances for **5** and **6** (1.975(4) and 1.976(4) Å, respectively) are slightly longer than in any of the **1**−**4** structures. The Fe−N_{ax} distances, 2.203(4), 2.269(5) Å and 2.262(4), 2.267(5) Å for **5** and **6**, respectively, are similar to each other and to the same distances in the molecular structures of **1**−**4** (see Table 2).

Solution magnetic susceptibility studies for all complexes were carried out using the Evans method[28,29] in CD_2Cl_2 in the temperature range from +35 to −93 °C with increments of 5 °C. The effective magnetic moment, μ_{eff}, of a methylene chloride solution of $[FeOETPP(4\text{-}CNPy)_2]ClO_4$ changes slightly with temperature according to the following linear dependence: $\mu_{eff} = (3.87 \pm 0.01) - (1.8 \pm 0.1) \times 10^{-3}\ T\ \mu_B$; $R = 99.0\%$, where R is the correlation coefficient (Figure 5 and Supporting Information Figure S3). It is characteristic of the $S = {}^3/_2$ state. SQUID magnetic susceptibility data above 200 K[20] support this observation. On the other hand, the effective magnetic moments of both $[FeOMTPP(4\text{-}CNPy)_2]ClO_4$ and $[FeTC_6TPP(4\text{-}CNPy)_2]ClO_4$ change drastically with temperature. In the case of $[FeOMTPP(4\text{-}CNPy)_2]ClO_4$, at all temperatures above 260 K, $\mu_{eff} = 3.56\ \mu_B$, somewhat lower than expected for the $S = {}^3/_2$ state (3.87 μ_B); however, this value depends on the assumption that there are no solvent molecules in the solid starting material, $(OMTPP)FeClO_4$ (unfortunately elemental analysis was not done on these complexes, which were, however, heated in a vacuum for 4 h before use). If there were one CH_2Cl_2 per formula unit, the μ_{eff} would be 3.73 μ_B, while if there were two it would be 3.91 μ_B. Ikeue and co-workers obtained a very similar temperature dependence, but with a limiting value of μ_{eff} of ∼4.3 μ_B.[10] This value seems high, as might be expected if there were some evaporation of the CD_2Cl_2 solvent during the measurements. Hence, there are probably inaccuracies in both measurements, meaning that the values of these solution measurements of μ_{eff} are probably only good

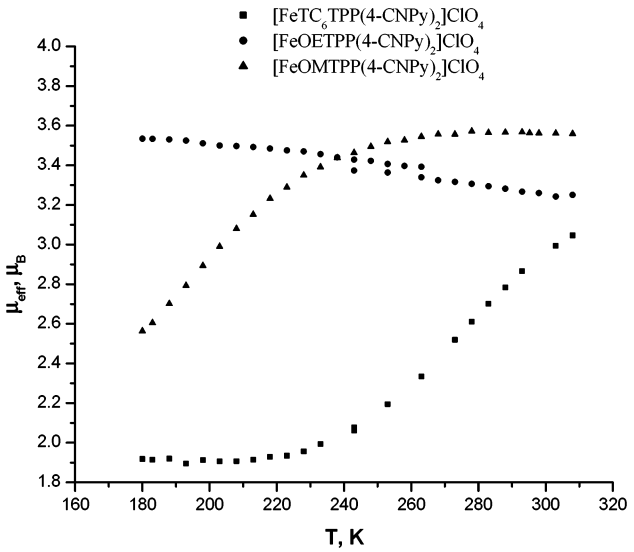

Figure 5. Temperature dependence of the effective magnetic moments, μ_{eff} for $[FeOMTPP(4\text{-}CNPy)_2]ClO_4$, $[FeOETPP(4\text{-}CNPy)_2]ClO_4$, and $[FeTC_6TPP(4\text{-}CNPy)_2]ClO_4$ in CD_2Cl_2 by the Evans method. In the case of $[FeOETPP(4\text{-}CNPy)_2]ClO_4$, the results are shown for experiments that were run on two different days. Slight inconsistency of data can be explained by some evaporation of the solvent during storage.

to ±10%. Despite this, the important point is that both studies show that the magnetic moment increases with temperature until it reaches a plateau characteristic of an $S = {}^3/_2$ complex at approximately 260 K. At lower temperatures the spin state decreases, but a pure LS state cannot be reached over the temperature range accessible to the liquid-state magnetic susceptibility measurements (>180 K). In the case of $[FeTC_6TPP(4\text{-}CNPy)_2]ClO_4$, above 230 K the complex is in transition from IS, $S = {}^3/_2$, to LS, $S = {}^1/_2$, and below 230 K the pure LS state is observed with its characteristic μ_{eff} of $1.95 \pm 0.05\ \mu_B$.

Proton NMR Studies of $[FeOMTPP(4\text{-}CNPy)_2]ClO_4$. An example of the 1D ^1H NMR spectrum of $[FeOMTPP(4\text{-}CNPy)_2]ClO_4$, at 203 K, is shown in Figure 6, together with the spectra for two other complexes of this study. Note that the spectra of the three complexes have different chemical shift scales due to the large difference in chemical shift ranges among the complexes. NMR experiments were carried out in the temperature range from 295 to 180 K. The stability of the bis(4-CNPy) complex of $(OMTPP)FeClO_4$ is extremely low, even in the presence of a large excess of 4-CNPy, and the kinetics of ligand exchange are extremely rapid. Thus, there are no free (F) or bound (L) 4-CNPy peaks in its NMR spectrum at 203 K, and the large downfield shift of the methyl resonances indicates that the majority of the molecules are in the $S = {}^3/_2$ state. At all temperatures above 198 K, no clear evidence of ligand binding occurs, and the temperature dependence of the chemical shifts for all protons is not linear (Supporting Information Figure S4A). Only below 198 K do broad free and bound 4-CNPy peaks begin to appear. Below that point, the temperature dependence of the chemical shifts becomes linear but does not extrapolate to the diamagnetic values at $T^{-1} = 0$ for all resonances. In 2D NOESY experiments carried out at 183 K (20 ms mixing time), strong chemical exchange cross-peaks between free (F) and bound (L) 3,5-H are observed (not shown), implying a high rate of ligand exchange (dissociation of bound ligand and binding of free 4-CNPy to OMTPPFe(III)) even at this low temperature. This is an unusual result, because in most iron(III) dodecasubstituted complexes with various pyridines and imidazoles, ligand exchange was undetectable on the NMR time scale below 203 K.[38,42] In the same NOESY experiment, NOE cross-peaks between phenyl protons are observed ($o-m$ and $m-p$). Peak assignment was based on 2D COSY and NOESY results, as well as on the integration of peaks in the 1D spectra and proton T_1 values. Peak assignments for two different temperatures, 193 and 180 K, together with relaxation times, T_1's, at 180 K are presented in Supporting Information Table S16, and chemical shifts of the protons of the complex are given at 243, 213, and 183 K in Table 4, together with those reported in ref 10. All T_1's (Supporting Information Table S16) are very short due to rapid chemical exchange between the spin states and the ligand on−off (dissociation/association) process.

Proton NMR Studies of $[FeOETPP(4\text{-}CNPy)_2]ClO_4$. Proton NMR studies were carried out in CD_2Cl_2 (from 180 to 303 K), $CDCl_3$ (from 303 to 330 K), and $C_2D_2Cl_4$ (from 303 to 363 K). Results are presented here for $[FeOETPP(4\text{-}CNPy)_2]ClO_4$ in CD_2Cl_2 unless otherwise stated. An example of the 1D ^1H spectrum, at 203 K, is shown in Figure 6. Chemical shifts and relaxation times at 233 and 193 K are presented in Supporting Information Table S17, and chemical shifts at 243, 213, and 183 K are presented in Table 4, along with those of other complexes of this study. In Table 4, the chemical shifts are also compared to those from refs 10 and 20, and it can be seen that several resonances (δ_{pyrr} for CH_2(in) and δ_o) are quite different for the two investigations of this complex. We will return to this point in the Discussion section. The temperature dependence of chemical shifts is displayed as a Curie plot in Supporting Information Figure S4B.

Because of rapid ligand exchange kinetics, the free (F) and bound ligand (L) peaks can be found only below 248 K. Even so, all resonances except CH_2(in) show linear temperature behavior on the Curie plot up to 330 K (in CD_2Cl_2 and $CDCl_3$), leading us to believe that at higher temperatures (from 243 to 330 K), despite rapid ligand exchange in the presence of 40 mM excess 4-CNPy, the porphyrin complex is bis(4-CNPy) ligated. Also in support of this conclusion is the fact that the proton NMR spectra of the perchlorate complex, in the absence of added 4-CNPy, are extremely broad and very different in appearance from the spectra in the presence of 4-CNPy; the chemical shifts of

(38) Yatsunyk, L. A. Ph.D. Dissertation, University of Arizona, 2003.
(39) Shokhirev, N. V.; Walker, F. A. *J. Phys. Chem.* **1995**, *99*, 17795−17804.
(40) http://www.shokhirev.com/nikolai/programs/prgsciedu.html.
(41) Yatsunyk, L. A.; Walker, F. A. Manuscript in preparation. The experiments for (OETPP)FeCl were done at three different magnetic field strengths, 300, 500, and 600 MHz, and in two different solvents, CD_2Cl_2 and $C_2D_2Cl_4$. All data can be described by single linear dependence. Thus, a solvation effect is not present.
(42) Ogura, H.; Yatsunyk, L.; Medforth, C. J.; Smith, K. M.; Barkigia, K. M.; Renner, M. W.; Melamed, D.; Walker, F. A. *J. Am. Chem. Soc.* **2001**, *123*, 6564−6578.

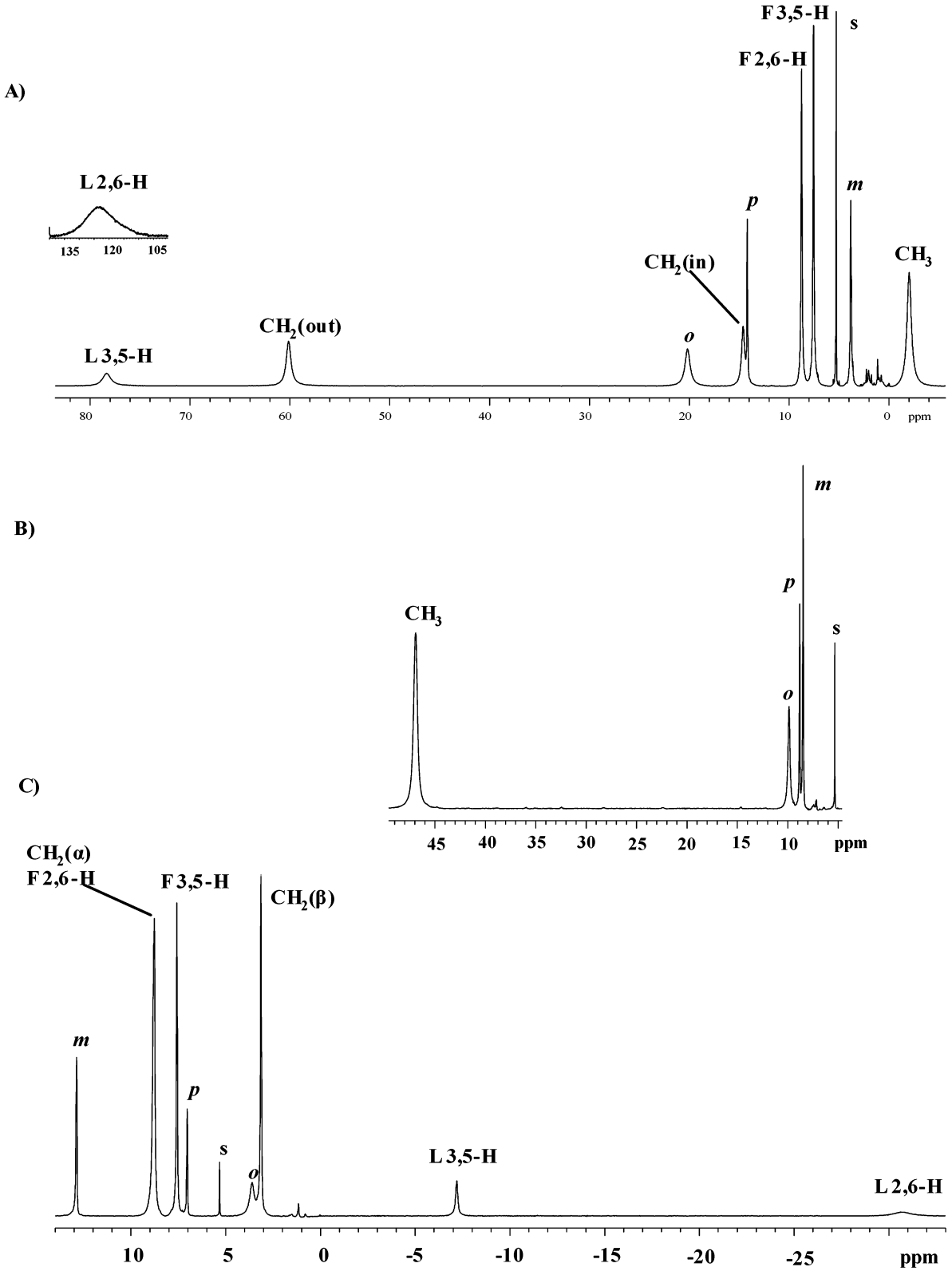

Figure 6. Proton NMR spectra of (a) $[FeOETPP(4\text{-}CNPy)_2]ClO_4$, (b) $[FeOMTPP(4\text{-}CNPy)_2]ClO_4$, and (c) $[FeTC_6TPP(4\text{-}CNPy)_2]ClO_4$ obtained in CD_2Cl_2 at 203 K. Note that each spectrum has a different scale since large differences in chemical shifts are observed for the three complexes. No free or bound 4-CNPy peaks are observed in the case of $[FeOMTPP(4\text{-}CNPy)_2]ClO_4$ due to the rapid kinetics of ligand exchange. $[FeOETPP(4\text{-}CNPy)_2]ClO_4$ is in the $S = {}^3/_2$ state with high downfield shifts for both ligand and CH_2(out) resonances and following the order for phenyl-H $\delta_o > \delta_p > \delta_m$. $[FeOMTPP(4\text{-}CNPy)_2]ClO_4$ is in transition from $S = {}^3/_2$ to LS with $S = {}^3/_2$ being predominant and is characterized by a large downfield shift of CH_3 (though smaller than for CH_2(out)) and the same order of phenyl resonances as in $[FeOETPP(4\text{-}CNPy)_2]ClO_4$. $[FeTC_6TPP(4\text{-}CNPy)_2]ClO_4$ is in the LS state with upfield shifts for L 2,6 and 3,5-H and $\delta_m > \delta_p > \delta_o$ order of phenyl resonances. Signal assignment: *o*, *m*, *p* correspond to *ortho*-, *meta*-, and *para*-phenyl-H; F and L indicate free and bound ligand peaks; s represents CH_2Cl_2.

Table 4. Chemical Shifts for Selected Resonances in $[FeOETPP(4\text{-}CNPy)_2]ClO_4$, $[FeOMTPP(4\text{-}CNPy)_2]ClO_4$, and $[FeTC_6TPP(4\text{-}CNPy)_2]ClO_4$, in CD_2Cl_2

porphyrin	δ_{pyrr}[a]	$\delta_{L3,5\text{-}H}$	$\delta_{L2,6\text{-}H}$	δ_m	δ_p	δ_o	$\delta_m - \delta_p$	$\delta_m - \delta_o$
				273 K				
OETPP	45.7, 14.0	—	—	5.0	12.5	17.2	−7.5	−12.2
	(—)[b]			(6.8)[b]	(10.4)[b]	(14.4)[b]		
	45.8, 17.2[c]			5.0[c]	12.5[c]	14.1[c]	−7.5[c]	−9.1[c]
OMTPP	67.8	—	—	6.8	10.3	13.5	−3.5	−6.7
	(76.0)[b]			(9.8)[b]	(7.3)[b]	(12.9)[b]		
	65.4[c]			6.6[c]	10.5[c]	13.8[c]	−3.9[c]	−7.2[c]
TC_6TPP	51.3	—	—	—	—	—	—	—
	(94.7,87.4)[b]			(10.2,9.6)[b]	(9.2)[b]	(13.3,10.6)[b]		
	62.1[c]			—[c]	8.2[c]	?[c]	—	—
				243 K				
OETPP	50.9, 14.2	66.0	103.4	4.6	13.2	18.3	−8.6	−13.7
	(—)[b]			(6.8)[b]	(10.4)[b]	(14.4)[b]		
OMTPP	65.8	—	—	6.7	10.4	13.6	−3.8	−6.9
	(76.0)[b]			(9.8)[b]	(7.3)[b]	(12.9)[b]		
TC_6TPP	21.5	—	—	11.1	7.3	5.3	+3.8	+5.8
	(94.7, 87.4)[b]			(10.2, 9.6)[b]	(9.2)[b]	(13.3, 10.6)[b]		
				213 K				
OETPP	57.5, 14.5	74.9	117.9	4.1	13.9	19.7	−9.8	−15.6
	(—)[b]			(6.6)[b]	(10.8)[b]	(15.4)[b]		
OMTPP	53.9	38.1[d]	49.4[d]	7.7	9.5	11.3	−1.7	−3.6
	(87.9)[b]			(10.1)[b]	(~7.2)[b]	(13.6)[b]		
TC_6TPP	10.4	−5.6	−27.8	12.5	7.1	3.9	+5.4	+8.6
	(110.4, 101.5)[b]			(10.2, 8.5)[b]	(9.5)[b]	(14.4, 11.0)[b]		
				183 K				
OETPP	66.1, 14.8	86.4	137.0	3.3	14.8	21.3	−11.5	−18.0
	(49.6, 92.6)[b]			(~6.3)[b]	(11.4)[b]	(~16)[b]		
	67.6, 21.7[c,e]			3.3[c,e]	15.0[c,e]	14.8[c,e]	−11.7[c,e]	−11.5[c,e]
OMTPP	31.4	14.9	2.9[d]	10.3	7.5	6.8	+2.9	+3.5
	(114, 94.4)[b]			(10.5)[b]	(~7.1)[b]	(14.6)[b]		
	30.2[c,e]			10.6[c,e]	7.4[c,e]	6.4[c,e]	+3.2[c,e]	+4.2[c,e]
TC_6TPP	6.8	−9.9	−35.5	13.7	7.0	2.9	+6.7	+10.8
	(123.7, 113.7)[b]			(10.2, 9.3)[b]	(9.7)[b]	(15.6, 11.5)[b]		
	13.3[c,e]			(no m-H)[c,e]	6.6[c,e]	4.0[c,e]	(no m-H)[c,e]	(no m-H)[c,e]

[a] δ_{pyrr} indicates CH_2(out) and CH_2(in), in that order, for OETPP, $CH_2(\alpha)$ for TC_6TPP, and CH_3 for OMTPP. [b] Chemical shifts for perchlorate complex, in CD_2Cl_2. [c] Taken from ref 10. [d] Calculated from the Curie plot (Figure S3A). [e] Reference 10, average of chemical shifts at 193 and 173 K.

the perchlorate complexes at four temperatures are included in Table 4. Intercepts at $T^{-1} = 0$ are close to diamagnetic values for the porphyrin CH_3 and phenyl (*o*, *m*, and *p*) resonances, indicating that the $S = {}^3/_2$ state is the only spin state accessible to this complex. In line with this, use of the 2-level temperature-dependent fitting program created by Dr. Nikolai V. Shokhirev in this laboratory[39,40] indicated that the temperature-dependence was best represented by a 1-level fit; i.e., there is no thermally accessible excited state.

Measurements of spin−lattice relaxation times, T_1's, were done at all temperatures. All resonances fit into one of two groups according to their T_1's. Protons of CH_2(out), CH_2(in), porphyrin CH_3, phenyl-*o*, L 3,5-H, and L 2,6-H belong to the first group, with very short T_1 values (1−10 ms). In fact, the T_1 of L 2,6-H was too short to obtain accurate measurements. Protons of phenyl-*m* and -*p* belong to the second group, with substantially longer T_1's (17−75 ms). In both groups, T_1 decreases either linearly or nearly so with decreasing temperature, except in the case of L 3,5-H, where a strongly curved decrease of T_1 is observed (see Supporting Information Figure S5). Relaxation times for F 2,6-H and F 3,5-H increase with decreasing temperature due to the common fact that in the absence of chemical exchange the T_1's of small molecules increase as the temperature is lowered.

Even at high temperatures two distinct resonances can be observed for the methylene protons of the ethyl groups, and both COSY and NOESY/EXSY spectra show the geminal and/or chemical exchange coupling of these protons; an example of chemical exchange coupling is shown in Figure 7. For an adjacent pair of ethyl groups, one resonance, CH_2-(out), is due to the methylene protons that point away from each other and toward the phenyl rings, and the other, CH_2-(in), is due to the protons that point toward each other. These peaks are good probes for studying ring inversion in $[FeOETPP(4\text{-}CNPy)_2]ClO_4$ using NOESY/EXSY techniques by measuring the volumes of diagonal and cross-peaks between these two methylene resonances. An example of the downfield part of the NOESY spectrum (288 K, 3 ms mixing time) is shown in Figure 7. Ring inversion is detectable on the NMR time scale only above 243 K and becomes very slow below this temperature.

Determination of the Rates of Porphyrin Ring Inversion for $[FeOETPP(4\text{-}CNPy)_2]ClO_4$. NOESY/EXSY data were obtained from experiments run on the complex containing the highest concentration of 4-CNPy, 82 mM, from 243 to 330 K in intervals of 5 K in CD_2Cl_2 and in $CDCl_3$. The diagonal- and cross-peak volumes of the methylene peaks were used to obtain rates of ring inversion and activation parameters for this process (see Experimental Section). Apart

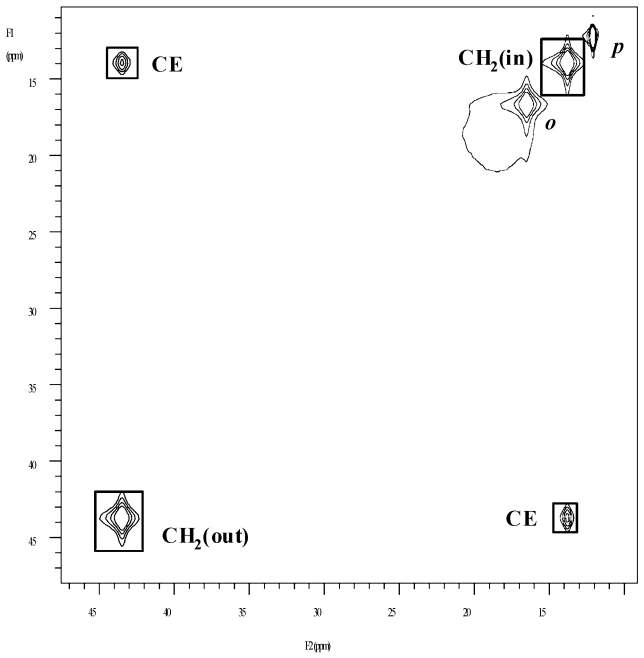

Figure 7. Downfield part of NOESY/EXSY spectrum of [FeOETPP(4-CNPy)$_2$]ClO$_4$ at 288 K in CD_2Cl_2. It was acquired with a spectral width of 20 kHz, 512 × 128 complex points, 80 transients per t_1 increment, a 3 ms mixing time, and 50 ms relaxation delay between scans. The spectrum was processed after application of Gaussian apodization (14 ms and 3 ms in the 1st and the 2nd dimension, respectively). Note that the spectral window is substantially broader than required by the spread of the proton resonances; this is due to the fact that the CH_2(out) peak is at the edge of the spectral window. It is attenuated due to resonance offset effect, and no accurate measurements of its volume can be obtained. Therefore, the spectral width was increased and transmitter offset was set to the position exactly between the two methylene peaks to ensure their equal excitation by the 90° ^{1}H pulse. Volumes of cross-peaks were measured within the boxes shown, and the average of the two equivalent cross-peaks was used.

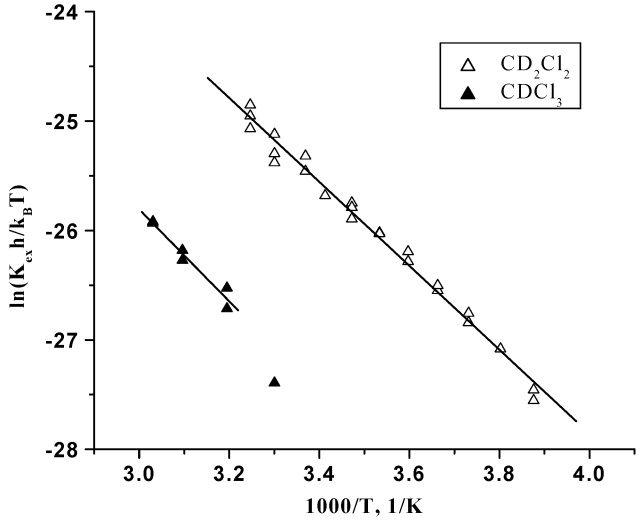

Figure 8. Eyring plot of the kinetic data obtained for the porphyrin ring inversion process in [FeOETPP(4-CNPy)$_2$]ClO$_4$ in CD_2Cl_2 and $CDCl_3$. Calculated values of $\Delta H^{\ddagger} = 32$ and 35 kJ mol^{-1} and $\Delta S^{\ddagger} = -104$ and -110 J mol^{-1} K^{-1} were determined for the ring inversion process in CD_2Cl_2 and $CDCl_3$, respectively.

from CE cross-peaks, strong NOE cross-peaks of negative phase (opposite to the phase of both diagonal peaks and CE cross-peaks) were observed between diastereotopic methylene protons over the temperature range of the NOESY experiments. This negative intensity decreases the volume of CE cross-peaks substantially in the case of slow ring inversion and results in underestimated rates of ring inversion. For this reason, points obtained for 243 and 253 K were not used for the calculation of kinetic parameters. Using peak volumes, the rate of ring inversion was calculated according to eq 3, and the results are presented in the form of an Eyring plot in Figure 8. Data obtained for two different solvents, CD_2Cl_2 and $CDCl_3$, show a small solvation effect. This is unlike the case of (OETPP)FeCl,[38,41] where no solvation effect was observed and data for two different solvents were described by one linear fit. However, an influence of solvent (CD_2Cl_2 vs $C_2D_2Cl_4$) on ring inversion activation parameters was observed for (F_{20}OETPP)FeCl.[38,41] According to the results obtained for [FeOETPP(4-CNPy)$_2$]ClO$_4$ in CD_2Cl_2 solution, the following activation parameters were determined: enthalpy, $\Delta H^{\ddagger} = 32.0(8)$ kJ mol^{-1}, entropy, $\Delta S^{\ddagger} = -104(3)$ J mol^{-1} K^{-1}, the free energy of activation, $\Delta G^{\ddagger}_{298} = 63(2)$ kJ mol^{-1}, and the rate of ring inversion at 298 K, $k_{ex}(298) = 59$ s^{-1}. The same parameters in $CDCl_3$ solvent are slightly different: $\Delta H^{\ddagger} = 35(4)$ kJ mol^{-1}, $\Delta S^{\ddagger} = -110(12)$ J mol^{-1} K^{-1}, $\Delta G^{\ddagger}_{298} = 68(7)$ kJ mol^{-1}, and $k_{ex}(298) = 8.6$ s^{-1}. The free energy of activation at 298 K is similar to that of other OETPPFe(III) complexes with planar aromatic axial ligands (55(3), 60(1), and 56(3) kJ mol^{-1} at 298 K for [F_{20}OETPP(4-Me$_2$NPy)$_2$]Cl, [FeOETPP-(1-MeIm)$_2$]Cl, and [FeOETPP(4-Me$_2$NPy)$_2$]Cl, respectively).[38,41] However, the entropy and enthalpy of activation differ substantially. $\Delta H^{\ddagger}$ is lower than that for any other OETPPFe(III) complex, which is probably due to the long Fe−N_{ax} bonds (2.167−2.240 Å) in [FeOETPP(4-CNPy)$_2$]-ClO$_4$ (vide supra) as compared to those in [FeOETPP-(1-MeIm)$_2$]Cl, (1.976(3) and 1.978(3) Å)[42] and [FeOETPP-(4-Me$_2$NPy)$_2$]Cl (1.984(5) and 2.099(12) Å).[42] Molecular mechanics calculations of the barrier of porphyrin ring inversion would be required in order to rationalize the results obtained.

The solvation effect is reflected not only in the activation parameters, but also in the relaxation times of protons and their chemical shifts in the different solvents, CD_2Cl_2, $CDCl_3$, and $C_2D_2Cl_4$ (see Supporting Information Table S18). The latter solvent was used in an attempt to obtain the rates of ring inversion at high temperatures, but due to weak binding of 4-CNPy and therefore extremely short relaxation times, T_1's, NOESY results were not meaningful under these conditions. T_1 relaxation times for protons in [FeOETPP(4-CNPy)$_2$]ClO$_4$ decrease with an increasing number of Cl atoms in the solvent molecule. However, there is no direct dependence of chemical shifts on the nature of the solvent; the values of chemical shifts differ by ≤2.5 ppm among the different solvents.

From 2D data,[43] it was found that ligand exchange becomes slow on the NMR (NOESY/EXSY) time scale below 203 K. The NOE crossover point for the NOESY spectra occurs at 223 K; below this temperature the NOE cross-peaks are positive (in phase with the diagonal peaks). As the temperature decreases, the NOE intensity increases:

for example, for methylene protons at 203 K the average volume of the NOE cross-peaks is 1.2% of the volume of the diagonal peak, while at 183 K it is 3.7%.[44]

Proton NMR studies of $[FeTC_6TPP(4\text{-}CNPy)_2]ClO_4$ were carried out over the temperature range from 295 to 180 K. It was found that the stability of the bis(4-CNPy) complex is relatively low and chemical exchange of ligands is rapid, so free (F) and bound (L) 4-CNPy peaks appear only below 223 K in the presence of 7.6 mM excess 4-CNPy (21 mM total). As the temperature is lowered, binding of 4-CNPy to $(TC_6TPP)FeClO_4$ becomes more favorable, and the exchange rate decreases. Finally, at 183 K, ligand exchange becomes undetectable on the NMR time scale in the NOESY experiments (there are no exchange cross-peaks between the bound and free ligand). Even at 183 K, however, all peaks in the spectra remain fairly broad.

An example of the 1D ^1H spectra for $[FeTC_6TPP(4\text{-}CNPy)_2]ClO_4$ is shown in Figure 6. Chemical shifts and relaxation times for all peaks at 213 and 183 K are presented in Supporting Information Table S19, and chemical shifts at 273, 243, 213, and 183 K are presented in Table 4, where they are compared to those of the other two complexes of this study and to those reported previously for a closely related complex, $[FeTBTXP(4\text{-}CNPy)_2]^+$.[10] As can be seen, there is a large difference in the α-CH_2 shifts and smaller differences in shifts for *o*-H and *p*-H resonances for the complex of this study and that reported previously.[10] The possible reasons for these differences will be considered below in the Discussion section. The temperature dependence of the chemical shifts is displayed in the form of a Curie plot (Supporting Information Figure S4C). Due to low complex stability, at relatively high temperatures all lines in the Curie plot are curved. Only the low temperature part of the graph (below 203 K), when the axial ligand is fully bound and the complex is fully low spin, is described by a straight line in all cases except for $CH_2(\alpha)$. Even so, diamagnetic intercepts ($T^{-1} = 0$) are only observed for the $CH_2(\beta)$ and phenyl-*p* protons. Detailed analysis of the temperature dependence is presented in the Discussion section.

The spin−lattice relaxation times, T_1's, were measured at all temperatures below 263 K. From 263 to 203 K, T_1 values increased for all peaks due to stronger ligand binding, and then, from 203 to 183 K, T_1 decreased for all peaks that are close to the paramagnetic center (see Supporting Information Table S19). The latter is the usual behavior for protons in paramagnetic complexes in the absence of chemical exchange.

Two-dimensional experiments were done in the temperature range from 233 to 183 K. In the NOESY spectra at all temperatures, two sets of CE cross-peaks are observed: F−L 3,5-H and F−L 2,6-H, indicating fast ligand exchange, which becomes NMR-undetectable below 183 K. This temperature is much lower than in the case of the $[FeTC_6TPP(4\text{-}Me_2NPy)]Cl$ complex, where ligand exchange becomes too slow to detect on the NMR time scale at 213 K.[38,41] Such a difference can be attributed to weaker basicity and binding ability of 4-CNPy as compared to 4-Me_2NPy. NOE cross-peaks are observed in the NOESY spectra between the phenyl-*m* and -*p*, and between $CH_2(\alpha)$ and $CH_2(\beta)$. Only weak NOE cross-peaks are observed between the phenyl-*m* and -*o* due to the extremely short relaxation time, T_1, of the phenyl-*o* protons (see Supporting Information Table S19).

Determination of the Rates of Porphyrin Ring Inversion for $[FeTC_6TPP(4\text{-}CNPy)_2]ClO_4$. Besides rapid ligand exchange, $[FeTC_6TPP(4\text{-}CNPy)_2]ClO_4$ undergoes fast ring inversion that is accompanied by ligand rotation. The presence of one $CH_2(\alpha)$ peak in all NMR spectra indicates that ring inversion is very rapid at all temperatures. In the limiting case of slow ring inversion, two resonances are expected for the diastereotopic $CH_2(\alpha)$ protons of this porphyrinate complex ($CH_2(\alpha)$-up for methylene protons that point toward the axial ligand and $CH_2(\alpha)$-down for the protons that point away from the axial ligand). However, lowering the temperature results only in broadening of the $CH_2(\alpha)$ peak: at 218 K the width of this peak is 31 Hz, but at 180 K it has broadened to 74 Hz. NMR spectra were taken every 3−5 K between these two temperatures. The data obtained can be used only for very rough estimation of the rate of ring inversion, since usually the $CH_2(\alpha)$ peak broadens to thousands of hertz, as in the case of $(TC_6TPP)FeCl$ and $[FeTC_6TPP(4\text{-}Me_2NPy)_2]Cl$,[38,41] before it splits into two resonances as the temperature is lowered further. Temperature dependence of the rate of ring inversion in $[FeTC_6TPP(4\text{-}CNPy)_2]ClO_4$ was estimated using the standard procedure of line shape analysis according to eq 4.[45] The temperature dependences of each component in eq 4, $\Delta\nu$, W^*, and W_0, have to be taken into account. Since W_0 is proportional to the rotational correlation time of the molecule (τ_c), which is in turn proportional to solvent viscosity (η/T), the line width of the $CH_2(\alpha)$ resonance was plotted against $1000\eta/T$ and the analytical expression for the inherent line width, W_0, (line width not influenced by chemical exchange) was obtained from linear fitting of the nearly flat, high temperature part of the plot (from 218 to 200 K): $W_0 = 24.66 + 2380\eta/T$. Extrapolation of this line into the regime where ring inversion becomes measurable on the NMR time scale (below 198 K) allows us to calculate the increase in line width, $W^* - W_0$, that is the due to the chemical exchange only, excluding the effect of increased solvent viscosity which slows molecular motion and also contributes to line broadening. However, since the sample cannot be cooled to the temperature where two different resonances for $CH_2(\alpha)$ are observed, the difference in chemical shift, $\Delta\nu$, cannot be measured. We have assumed that the minimum $\Delta\nu$ must be at least as large as the maximum line width (74 Hz) at 180 K (in reality values of $\Delta\nu$ at least as high as 1000 Hz could be expected). If larger values of $\Delta\nu$ are considered, the calculated rate constant would simply be scaled by the

(43) Only NOESY experiments were carried out since the spectral window was too broad for the performance of any spin-lock experiments such as ROESY or TOCSY.

(44) The NOE effect was measured as the following ratio: $V(CH_2(\text{out})\text{-cross})/V(CH_2(\text{out})\text{diagonal})$.

(45) Polam, J. R.; Shokhireva, T. Kh.; Raffi, K.; Simonis, U.; Walker, F. A. *Inorg. Chim. Acta* **1997**, *263*, 109−117.

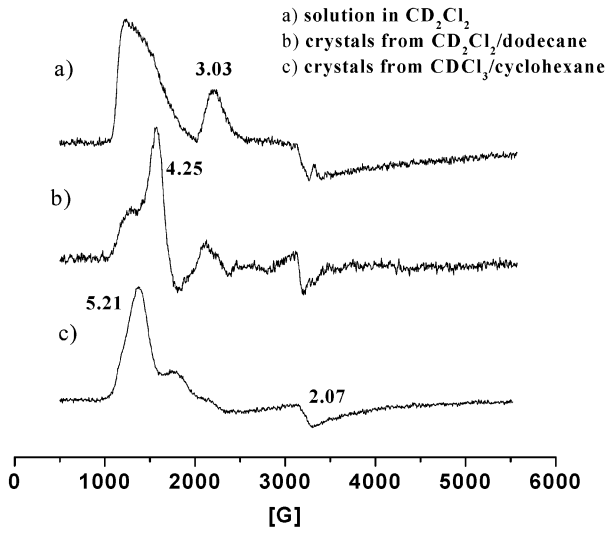

Figure 9. 4.2 K EPR spectra of $[FeOETPP(4\text{-}CNPy)_2]ClO_4$ (a) in a frozen CD_2Cl_2 solution, (b) as a polycrystalline sample obtained from CD_2Cl_2/dodecane, and (c) as a polycrystalline sample obtained from the $CDCl_3$/cyclohexane. The g values of 5.21, 4.25, and 2.07 are characteristic of the intermediate spin state, $S = {}^3/_2$, while $g = 3.03$ suggests LS with $(d_{xy})^2(d_{xz},d_{yz})^3$ configuration. All spectra have the same basic features with different intensity of signals.

constant quantity of $(\Delta\nu/74)^2$, and as a result, our assumption would not affect $\Delta H^{\ddagger}$, although it will affect $\Delta S^{\ddagger}$ and k_{ex}.

With the assumption that $\Delta\nu = 74$ Hz, the temperature dependence of k_{ex} was obtained in the range from 193 to 180 K, and an Eyring plot was constructed (Supporting Information Figure S6). Linear fitting of the data resulted in the following kinetic parameters: $\Delta H^{\ddagger} = 24(4)$ kJ mol^{-1}, $\Delta S^{\ddagger} = -20(21)$ J mol^{-1} K^{-1}, $\Delta G^{\ddagger}_{298} = 30(10)$ kJ mol^{-1}, and the minimum rate, k_{ex}, of 3.8×10^7 s^{-1} at 298 K. For comparison, ambient temperature rates of ring inversion in $(TC_6TPP)FeCl$ and $[FeTC_6TPP(4\text{-}Me_2NPy)_2]Cl$ are 4.4×10^7 and 2.8×10^7 s^{-1}, respectively.[38,41] Substantially smaller broadening of the $CH_2(\alpha)$ peak in $[FeTC_6TPP(4\text{-}CNPy)_2]ClO_4$ as compared to the same peak for the chloride or bis(4-Me_2NPy) analogues[38,41] indicates that the rate of ring inversion in the bis(4-CNPy) complex should be at least as high as 4.4×10^7 s^{-1}. This is about a million times faster than for $[FeOETPP(4\text{-}CNPy)_2]ClO_4$ in CD_2Cl_2 at the same temperature (vide supra).

EPR Studies of Polycrystalline and Solution Samples of $[FeOETPP(4\text{-}CNPy)_2]ClO_4$, $[FeOMTPP(4\text{-}CNPy)_2]ClO_4$, and $[FeTC_6TPP(4\text{-}CNPy)_2]ClO_4$. The EPR spectra of a frozen solution and two polycrystalline samples of $[FeOETPP(4\text{-}CNPy)_2]ClO_4$ are shown in Figure 9. All three spectra have the same basic features, with $g = 5.21$, 4.25, 3.03, and 2.07. Ikeue and co-workers report somewhat different g-values of this complex of 4.28, 3.80, and 2.08.[20] The signals with g values larger than 4, plus the value near 2.0, are characteristic of the intermediate ($S = {}^3/_2$) spin state, while the $g = 3.03$ peak is typical of low spin (LS) ferrihemes. However, it is not accompanied by other features indicative of LS Fe(III) and, thus, may indicate a single feature "large g_{max}" signal similar to those observed for other lower-basicity pyridine complexes of TMPFe(III) with unusually low g_{max} values.[5] $[FeOMTPP(4\text{-}CNPy)_2]ClO_4$ and $[FeTC_6TPP(4\text{-}CNPy)_2]CO_4$ both have typical axial-type EPR spectra with $g_{\perp} = 2.49$, $g_{\parallel} = 1.6$ (Supporting Information Figure S7), characteristic of the LS Fe(III) $(d_{xz},d_{yz})^4(d_{xy})^1$ ground state;[5,6,8,10] these g-values have previously been reported as 2.52 and 1.82 for $[FeOMTPP(4\text{-}CNPy)_2]^+$ and 2.49 and unresolved for $[FeTBTXP(4\text{-}CNPy)_2]^+$.[10]

Discussion

Spin States of the Complexes. The EPR data indicate that at 4.2 K both $[FeOMTPP(4\text{-}CNPy)_2]ClO_4$ and $[FeTC_6TPP(4\text{-}CNPy)_2]ClO_4$ complexes are low spin (LS) with axial EPR signals ($g_{\perp} = 2.49$, $g_{\parallel} = 1.60$) that are characteristic of the $(d_{xz},d_{yz})^4(d_{xy})^1$ electronic ground state. Similar EPR spectra are observed for bis(4-cyanopyridine)iron(III) complexes with various porphyrinates, TMP ($g_{\perp} = 2.53$, $g_{\parallel} = 1.56$),[5] TPP ($g_{\perp} \geq 2.62$, $g_{\parallel} \leq 0.92$),[6] T^nPrP ($g_{\perp} = 2.46$, $g_{\parallel} = 1.68$),[8] T^cPrP ($g_{\perp} = 2.49$, $g_{\parallel} = 1.58$),[8] T^iPrP ($g_{\perp} = 2.41$, $g_{\parallel} = 1.79$),[8] OMTPP ($g_{\perp} = 2.52$, $g_{\parallel} = 1.82$),[10] and TBTXP ($g_{\perp} = 2.49$, $g_{\parallel}$ not observed).[10] Iron(III) porphyrinate complexes with other weak σ-basicity or π-acceptor axial ligands (Py, 3-CNPy, CN^-, t-BuNC) display axial EPR spectra, as well.[5,8−10,46] Utilizing the proper axis definition of Taylor[11] ($g_{zz} = -g_{\parallel}$, $g_{yy} = -g_{xx} = g_{\perp}$), the crystal field splittings for bis(4-cyanopyridine)iron(III) complexes were calculated from the EPR data. The rhombicity, V/λ, is always 0.0 due to degeneracy of the filled d_{xz}, d_{yz} orbitals, and the tetragonality, Δ/λ, is −3.12, −3.12, −2.92, −1.72, −3.50, −3.05, and −4.26 for OMTPP, TC_6TPP (both this work), TMP,[5] TPP,[6] T^nPrP,[8] T^cPrP,[8] and T^iPrP,[8] respectively. The absolute value of the tetragonality, $|\Delta/\lambda|$, for representative bis(t-BuNC) (a good π-acceptor) complexes is substantially higher (6.93−11.3).[9,46−48] The relatively small values of the tetragonality for bis(4-CNPy)iron(III) complexes indicates a much smaller splitting of the former t_{2g} orbitals (the d_{xy} orbital is only 2.9−4.3λ higher than d_{xz},d_{yz}) and a possible switch to the other LS electron configuration, $(d_{xy})^2(d_{xz},d_{yz})^3$. On the other hand, the large difference in the energy between the d_{xy} and d_{xz},d_{yz} orbitals of the bis(t-BuNC) porphyrin complexes ensures the $(d_{xz},d_{yz})^4(d_{xy})^1$ ground state at all temperatures. On the basis of the EPR data for $[FeOMTPP(4\text{-}CNPy)_2]ClO_4$ and $[FeTC_6TPP(4\text{-}CNPy)_2]ClO_4$, we have also calculated the values of the mixing coefficients a, b, and c for the wave functions d_{xz}, d_{yz}, and d_{xy}, respectively: $a = b = 0.1712$, and $c = 0.9577$; thus $c^2 = 0.9172$ and $a^2 + b^2 + c^2 = 0.9758$, indicating the need for an orbital reduction factor, k, of 1.025. As a result, the ground states of $[FeOMTPP(4\text{-}CNPy)_2]ClO_4$ and $[FeTC_6TPP(4\text{-}CNPy)_2]ClO_4$ have 94% d_{xy} character at 4.2 K. It is noteworthy that the $\sum g^2$ for bis(4-CNPy) iron(III) porphyrin complexes (14.58−15.2)[5,6,9] is far from the theoretical value of 16, indicating partial quenching of orbital angular momentum in the $(d_{xz},d_{yz},)^4(d_{xy})^1$ ground state configuration. However, the g-values reported by Ikeue et al.[10]

(46) Yatsunyk, L. A.; Walker, F. A. Submitted for publication.
(47) Walker, F. A.; Nasri, H.; Turowska-Tyrk, I.; Mohanrao, K.; Watson, C. T.; Shokhirev, N. V.; Debrunner, P. G.; Scheidt, W. R. *J. Am. Chem. Soc.* **1996**, *118*, 12109−12118.
(48) Simonneaux, G.; Schünemann, V.; Morice, C.; Carel, L.; Toupet, L.; Winkler, H.; Trautwein, A. X.; Walker, F. A. *J. Am. Chem. Soc.* **2000**, *122*, 4366−4377.

for $[FeOMTPP(4\text{-}CNPy)_2]^+$ (2.52, 1.82) lead to $\sum g^2 = 16.013$, indicating no quenching of orbital angular momentum. These values are different from the ones obtained in this study (2.49, 1.60, $\sum g^2 = 14.960$).

The solution magnetic susceptibility data for $[FeOMTPP(4\text{-}CNPy)_2]ClO_4$ and $[FeTC_6TPP(4\text{-}CNPy)_2]ClO_4$ at the lowest temperatures accessible in the liquid state are in good agreement with the EPR results. In the case of $[FeTC_6TPP(4\text{-}CNPy)_2]ClO_4$, a pure LS, $S = {}^1/_2$, state occurs below 240 K with $\mu_{eff} = 1.95 \pm 0.05\ \mu_B$, indicative of little orbital contribution and consistent with the $(d_{xz},d_{yz},)^4(d_{xy})^1$ ground state detected in the 4.2 K EPR spectra. Even though in the $[FeOMTPP(4\text{-}CNPy)_2]ClO_4$ case the pure LS state cannot be achieved over the temperature range accessible to the solution magnetic measurements, on the basis of the magnetic data (Figure 5) we can predict that this complex adopts a predominantly LS state at temperatures below 150−140 K and, as a result, exhibits an axial EPR signal at 4.2 K. As the temperature is raised, the population of the $S = {}^3/_2$ state increases, and above 260 K, $[FeOMTPP(4\text{-}CNPy)_2]ClO_4$ exists exclusively in the $S = {}^3/_2$ state with $\mu_{eff} = 3.56 \pm 0.36\ \mu_B$. An $S = {}^3/_2$ state for $[FeTC_6TPP(4\text{-}CNPy)_2]ClO_4$, however, is never achieved, and even at 320 K, this complex is still in spin equilibrium ($S = {}^1/_2 \leftrightarrow S = {}^3/_2$). Transition from the LS to the $S = {}^3/_2$ state is attributed to the weak ligand field strength of the 4-CNPy ligand, which places both $[FeOMTPP(4\text{-}CNPy)_2]ClO_4$ and $[FeTC_6TPP(4\text{-}CNPy)_2]ClO_4$ very close to the spin crossover point ($S = {}^3/_2 \leftrightarrow S = {}^1/_2$).

On the other hand, $[FeOETPP(4\text{-}CNPy)_2]ClO_4$ has a completely different type of EPR spectrum at 4.2 K, with the following g values for the solid samples (Figure 9): 5.21, 4.25, 3.03, and 2.07. Both the CD_2Cl_2 frozen solution and polycrystalline samples display the same type of EPR signal, but with different relative intensities of the peaks (Figure 9). The EPR signals with g larger than 4 and around 2 point to the $S = {}^3/_2$ state, but $g = 3.03$ is likely a "large g_{max}" signal characteristic of the LS $(d_{xy})^2(d_{xz},d_{yz},)^3$ ground state, which is different from the LS electronic ground state of either the OMTPP or TC_6TPP complexes. There are several arguments that support this suggestion. First, the $g = 3.03$ value is very similar to the unusually low g_{max} values of 2.89, 3.07, and 3.17 observed in the EPR spectra of $[FeTMP(3\text{-}EtPy)_2]ClO_4$, $[FeTMP(3\text{-}ClPy)_2]ClO_4$, and $[FeTMP(2\text{-}MeHIm)_2]ClO_4$, respectively.[5] Therefore, there must be, especially in the frozen solution where the $g = 3.03$ signal is the most intense, some molecules of $[FeOETPP(4\text{-}CNPy)_2]ClO_4$ in the LS state. Low temperature SQUID measurements of solid samples do indicate that $[FeOETPP(4\text{-}CNPy)_2]ClO_4$ is a mixture of the $S = {}^1/_2$ and ${}^3/_2$ states below 200 K and that the population of the LS ($S = {}^1/_2$) state increases as the temperature is lowered.[20] Therefore, it is not surprising that in frozen solution at 4.2 K a detectable amount of LS ($S = {}^1/_2$) molecules of $[FeOETPP(4\text{-}CNPy)_2]ClO_4$ is observed in the EPR spectra. Second, the presence of the $g = 3.03$ signal in the EPR spectra of the polycrystalline sample can be justified by the fact that $[FeOETPP(Py)_2]ClO_4$ undergoes spin transition upon lowering the temperature from 298 to 180 K and then to 80 K.[21] Therefore, it is possible that freezing the $S = {}^3/_2$ state polycrystalline sample of $[FeOETPP(4\text{-}CNPy)_2]ClO_4$ in an EPR tube to 4.2 K leads to spin change for some molecules and as a result, a "large g_{max}" signal, especially, taking into account that no other geometry changes, except shortening of $Fe-N_{ax}$ bonds, is required. Of course, one would have expected that the LS state of $[FeOETPP(4\text{-}CNPy)_2]ClO_4$ should have the $(d_{xz},d_{yz},)^4(d_{xy})^1$ rather than the $(d_{xy})^2(d_{xz},d_{yz},)^3$ electronic configuration; however, neither we nor others[20] have observed an axial signal ($g_\perp \sim 2.6-2.5$, $g_{||} \sim 1.6$) in the EPR spectrum of $[FeOETPP(4\text{-}CNPy)_2]ClO_4$, but rather, we observed the "large g_{max}" signal. Finally, another argument in support of the $(d_{xy})^2(d_{xz},d_{yz},)^3$ ground state is that the saddled deviation of $[FeOETPP(4\text{-}CNPy)_2]ClO_4$ is the highest among OETPP, OMTPP, and TC_6TPP complexes and probably one of the highest observed thus far, and as was pointed out earlier,[9] saddled complexes appear to resist switching to the $(d_{xz},d_{yz},)^4(d_{xy})^1$ ground state. The EPR spectrum for $[FeOETPP(4\text{-}CNPy)_2]ClO_4$ was reported previously with somewhat different g values of 4.28, 3.80, and 2.08.[20]

To summarize, it is shown in this work and by others[5,6,9,10] that the stability of the $(d_{xz},d_{yx})^4(d_{xy})^1$ state in bis(4-CNPy) iron(III) complexes increases in the order OETPP ≪ TPP < TMP ≤ OMTPP ∼ TC_6TPP ∼ T^cPrP < T^nPrP < T^iPrP.

On the basis of 4.2 K EPR spectra, we also suggest that the LS ground state in $[FeOETPP(4\text{-}CNPy)_2]^+$, observed for a minor population of molecules, has the $(d_{xy})^2(d_{xz},d_{yz})^3$ configuration. Hence, EPR and solution magnetic susceptibility measurements are in good agreement with each other.

^{1}H NMR Studies of $[FeOETPP(4\text{-}CNPy)_2]ClO_4$, $[FeOMTPP(4\text{-}CNPy)_2]ClO_4$, and $[FeTC_6TPP(4\text{-}CNPy)_2]ClO_4$. The first observation made in the NMR studies was that the binding constant of 4-CNPy decreases in the order OETPP > TC_6TPP > OMTPP. Free ligand peaks are observed below −30, −50, and −75 °C for OETPP, TC_6TPP, and OMTPP, respectively, in the presence of a high molar excess of 4-CNPy. In accord with that, ligand exchange becomes slow on the NMR time scale at −70, −90, and much below −93 °C for OETPP, TC_6TPP, and OMTPP, respectively. Despite this, we were able to obtain crystals of $[FeOMTPP(4\text{-}CNPy)_2]ClO_4$, but any attempts to obtain crystals of $[FeTC_6TPP(4\text{-}CNPy)_2]ClO_4$ resulted in the five-coordinate perchlorate or nitrate complexes. In general, we found it difficult to obtain crystals of $[FeTC_6TPP(L)_2]^+$ with any of the axial ligands, and only one structure, of $[FeTC_6TPP(1\text{-}MeIm)_2]Cl$, has been reported.[18]

The second observation relates to the data of Table 4, where it can be seen that while the chemical shifts of $[FeOMTPP(4\text{-}CNPy)_2]^+$ at 273 and 183 K are within the deviations expected on the basis of calibration of the temperature controllers of two different NMR spectrometers, those for $[FeOETPP(4\text{-}CNPy)_2]^+$ (this work and refs 10 and 20) and $[FeTC_6TPP(4\text{-}CNPy)_2]^+$ (this work) or $[FeTBTXP(4\text{-}CNPy)_2]^+$ (ref 10) differ dramatically for some of the resonances. Notably, for $[FeOETPP(4\text{-}CNPy)_2]^+$, while the chemical shift of CH_2(out) is fairly similar at all common temperatures, that of CH_2(in) differs by 3 ppm at 273 K and 6.9 ppm at 183 K. Marked differences in the chemical shifts

of the *ortho*-phenyl protons are also observed (Table 4). The most likely explanation of these differences between the currently reported shifts and those reported previously[10] is that the previous study incorrectly assigned the two types of resonances, CH_2(in) and *o*-H. It is hard to imagine how this error could have been made, when simple COSY and NOESY/EXSY experiments available on all modern NMR spectrometers allow ready assignments of the resonances involved. Thus, the assignments of the present work are unambiguously the correct ones.

For $[FeTC_6TPP(4\text{-}CNPy)_2]^+$ it can also be seen from Table 4 that there are marked differences in the chemical shifts of the α-CH_2 protons from those reported for $[FeTBTXP(4\text{-}CNPy)_2]^+$.[10] These two compounds differ only in the fact that the latter compound has two *meta*-OCH_3 groups on each phenyl ring, and while these substituents might cause minor shifts in the *o*-H and *p*-H resonances, it seems unlikely that they would dramatically affect the ring conformation of the cyclohexenyl rings and thus the chemical shift of the α-CH_2 resonance from that observed in the present study of $[FeTC_6TPP(4\text{-}CNPy)_2]^+$. Nevertheless, at 273 K the chemical shift of the complex of the previous study is nearly 10 ppm larger than that of the present study, and even at 183 K the chemical shifts of the α-CH_2 protons in the two studies differ by 6.5 ppm (Table 4). We have included in Table 4 the chemical shifts of the perchlorate complexes of the three porphyrinates of this study, all of which have $S = {}^3/_2$ electronic states throughout the temperature range studied. While the direction of shift of the α-CH_2 proton resonance of ref 10 is that expected if not enough axial ligand had been added, the authors used 64 equiv of axial ligand, which, at 10 mM concentration of iron porphyrinate, should have been enough to ensure full complexation, especially at the lowest temperatures. Thus, we do not have an explanation for the differences in chemical shifts of the α-CH_2 protons of these two complexes.

In this work, ^{1}H NMR and solution magnetic susceptibility data were acquired over the same temperature range, and the results correlate extremely well. As discussed above, $[FeOETPP(4\text{-}CNPy)_2]ClO_4$ is in the $S = {}^3/_2$ state at all temperatures from ambient down to 180 K, $[FeOMTPP(4\text{-}CNPy)_2]ClO_4$ is in the $S = {}^3/_2$ state from ambient temperature to 240 K and then the LS state becomes populated as the temperature decreases, and, finally, $[FeTC_6TPP(4\text{-}CNPy)_2]ClO_4$ is in the LS state at any temperature below 230 K.

In the case of the $(d_{xz},d_{yz})^4(d_{xy})^1$ electronic ground state, the d_π orbitals are filled, but the d_{xy} unpaired electron can engage in spin delocalization to the porphyrinate ring if it is ruffled, and such ruffling is quite extreme in most of the complexes with the $(d_{xz},d_{yz})^4(d_{xy})^1$ electron configuration.[5,6,9,10,46−48] Such spin delocalization results in a large positive spin density at the *meso*-carbons, which leads to a large and positive difference in the chemical shifts of the phenyl protons (protons attached directly to the phenyl rings), $\delta_m - \delta_p$, and $\delta_m - \delta_o$, or to the following order of chemical shifts: $\delta_m > \delta_p > \delta_o$.[15] In the case of saddled porphyrins, *meso*-phenyl shifts are much smaller because of the reduced possibility of ruffling of the porphyrinate ring, and, therefore, smaller spin delocalization to the *meso*-carbons,[46] even though the EPR spectra indicate just as pure a $(d_{xz},d_{yz})^4(d_{xy})^1$ ground state for these 4-CNPy complexes as in the cases of ruffled iron porphyrinates.[5,6,8,10] When the ^{1}H NMR results are considered for $[FeOMTPP(4\text{-}CNPy)_2]ClO_4$, $\delta_m - \delta_p$ and $\delta_m - \delta_o$ are equal to −1.7 and −3.6 ppm at 213 K, and +2.9 and +3.5 ppm at 183 K (see Table 4). In comparison, the highly ruffled $[FeTPP(4\text{-}CNPy)_2]^+$ complex has much larger values of $\delta_m - \delta_p$ and $\delta_m - \delta_o$ of +5.7 and +14.2 ppm at 213 K.[15,16] Smaller $\delta_m - \delta_p$ and $\delta_m - \delta_o$ values, as compared to the same values in complexes with the $(d_{xz},d_{yz})^4(d_{xy})^1$ ground state stabilized by a ruffled porphyrin core, are indicative of poorer spin delocalization to the *meso*-carbons due to the purely saddled conformation expected for $[FeOMTPP(4\text{-}CNPy)_2]ClO_4$ in solution on the basis of its crystal structure. A substantial degree of ruffling is required for good interaction of the d_{xy} orbital with the porphyrin $a_{2u}(\pi)$ orbital.[6] In the case of $[FeTC_6TPP(4\text{-}CNPy)_2]ClO_4$, $\delta_m - \delta_p$ and $\delta_m - \delta_o$ are equal to +5.4 and +9.5 ppm at 213 K and +6.7 and +10.8 ppm at 183 K. These differences are larger than in the case of $[FeOMTPP(4\text{-}CNPy)_2]ClO_4$, pointing to higher (+) spin density at the *meso*-carbons, probably due to a significant ruffling of the TC_6TPP core. Although we were not able to obtain the structure of $[FeTC_6TPP(4\text{-}CNPy)_2]ClO_4$, structures of other complexes, $[FeTC_6TPP(1\text{-}MeIm)_2]Cl$[18] and $(TC_6TPP)FeCl$,[38] suggest ∼0.6:0.4 of saddled versus ruffled components are certainly possible in the core geometry.

In comparison, for $[FeOETPP(4\text{-}CNPy)_2]ClO_4$ at any temperature, the order of the phenyl shifts is $\delta_o > \delta_p > \delta_m$ (Table 4). This is the same order as for $[FeOMTPP(4\text{-}CNPy)_2]ClO_4$ at temperatures higher than 198 K (Figure 6). The phenyl shift differences $\delta_m - \delta_p$ and $\delta_m - \delta_o$ are large and negative at all temperatures (Table 4), indicating a fairly large negative spin density at the *meso*-carbons (i.e., the opposite sign as compared to the spin density on the metal).[15] The values of $\delta_m - \delta_p$ and $\delta_m - \delta_o$, extrapolated to 298 K (−7.3 and −11.6 ppm, respectively), are somewhat smaller in magnitude (70% and 90%, respectively) but opposite in sign to those for the $(d_{xz},d_{yz})^4(d_{xy})^1$ electron configuration complex $[FeTPP(t\text{-}BuNC)_2]^+$ [49] and of comparable magnitude but opposite in sign to those for $[FeTPP(4\text{-}CNPy)_2]^+$ [16] (128% and 82%, respectively), where there is significant spin delocalization to the $3a_{2u}(\pi)$ orbital. These values are about 17% and 24% of those observed for the HS Fe(III) porphyrin radical $[TPP{\cdot}FeCl]^+$,[50,51] and 33% and 42% of those observed for the IS ($S = {}^3/_2$) Fe(III) corrolate radical, [TPCorrFeCl],[52] suggesting, in analogy to what was found in the latter case, a partial $S = 2$ Fe(II), $S = {}^1/_2$ π-cation radical resonance structure, with antiferromagnetic coupling between metal and porphyrin unpaired electrons; antiferromagnetic coupling would thus result from the presence of

(49) Simonneaux, G.; Hindre, F.; Le Plouzennec, M. *Inorg. Chem.* **1989**, *28*, 823−825.
(50) Phillippi, M. A.; Goff, H. M. *J. Am. Chem. Soc.* **1982**, *104*, 6026−6034.
(51) Gans, P.; Marchon, J.-C.; Reed, C. A.; Regnard, J.-R. *Nouv. J. Chim.* **1981**, 203−204.
(52) Cai, S.; Licoccia, S.; D'Ottavi, C.; Paolesse, R.; Nardis, S.; Bulach, V.; Zimmer, B.; Shokhireva, T. Kh.; Walker, F. A. *Inorg. Chim. Acta* **2002**, *339C*, 171−178.

an unpaired electron in the $d_{x^2-y^2}$ orbital of HS iron(II), which has the proper symmetry to interact with the $3a_{2u}(\pi)$ orbital of the porphyrin ring when the latter is saddled.[53] This suggestion is further supported by arguments presented in the following four paragraphs.

Sakai and co-workers have pointed out that there are two possible electron configurations for $S = {}^3/_2$ iron porphyrinates, those being $(d_{xz},d_{yz})^3(d_{xy})^1(d_{z^2})^1$ and $(d_{xy})^2(d_{xz},d_{yz})^2(d_{z^2})^1$.[54] Qualitatively, the main difference expected in the NMR spectra is that the latter should have larger pyrrole-substituent shifts than the former (due to having two d_π unpaired electrons rather than one), and zero spin density at the *meso* positions (due to the absence of an unpaired electron in the d_{xy} orbital), while the former might have spin density at those positions if the porphyrinate ring is ruffled.[15] While it is indeed true that these two electron configurations are both possible and that the latter should have larger spin density at the pyrrole positions than the former (and we considered this possibility as the explanation of the large pyrrole-CH_2 shifts observed and discussed below before noticing the negative phenyl shift differences $\delta_m - \delta_p$ and $\delta_m - \delta_o$), neither of these electron configurations can explain the negative phenyl-H shift differences observed (or the exceptionally large pyrrole-CH_2 shifts observed for [FeOETPP-(4-CNPy)$_2$]ClO_4 discussed below and shown in Table 4). Thus, these negative phenyl-H shift differences indicate that something quite different is involved, i.e., spin transfer from the porphyrinate ring to the iron to create a partial π-cation radical, and further suggest the need for DFT calculations to be carried out on this system[15,55] to determine the extent of electron transfer from porphyrinate to iron in this complex.

The $S = {}^3/_2$ state is characterized by large upfield shifts for directly bound pyrrole protons,[15] which corresponds to large downfield shifts for protons of methyl or methylene groups directly attached to the pyrrole β-carbons.[15] This is observed in the case of the [FeOETPP(4-CNPy)$_2$]ClO_4 complex by average CH_2 shifts of 32.6 and 40.5 ppm at 243 and 183 K, respectively, and a positive slope of the temperature dependence of the CH_2(out) chemical shift on the Curie plot and small temperature dependence of the CH_2-(in), both of which extrapolate to close to the average diamagnetic CH_2 shift (2.3 ppm) at infinite temperature (Supporting Information Figure S4B), indicating no thermally accessible excited state is involved. A closer look at the average CH_2 shifts of [FeOETPP(4-CNPy)$_2$]ClO_4, as compared to those of the $S = {}^1/_2$ complex [FeOETPP-(4-Me$_2$NPy)$_2$]Cl (+8.1 and +7.8 ppm at 243 and 183 K, respectively[38]), both in CD_2Cl_2, shows that the 4-CNPy complex has anomalously large pyrrole-CH_2 shifts for a complex expected to have two d_π unpaired electrons for the $S = {}^3/_2$ state with electron configuration $(d_{xy})^2(d_{xz},d_{yz})^2(d_{z^2})^1$, as compared to the $S = {}^1/_2$ $(d_{xy})^2(d_{xz},d_{yz})^3$ electron configuration complex [FeOETPP(4-Me$_2$NPy)$_2$]Cl: If one d_π unpaired electron gives rise to an average isotropic shift of 8.1 − 2.3 = 5.8 ppm for this porphyrinate, then two would be expected to give rise to an isotropic shift of about double this amount, or a chemical shift of $2 \times 5.8 + 2.3 = 13.9$ ppm. The third unpaired electron of this IS state is expected to be in the d_{z^2} orbital, which will not contribute to the isotropic shifts of the porphyrin protons (although it certainly will contribute to those of the axial ligand protons in this 6-coordinate complex, as discussed below). However, instead of an average chemical shift of the CH_2 protons of 13.9 ppm at 243 K, the observed average shift is 32.6 ppm. A similar (somewhat larger) average CH_2 chemical shift is shown by the $S = {}^3/_2$, ${}^5/_2$ complex OETPPFeCl (44 ppm at 243 K[38]), which has been shown to be largely HS (90−96%),[56] with the downfield-shifted average CH_2 resonance thus resulting from σ-spin delocalization to the β-carbons arising from nearly full occupation of the $d_{x^2-y^2}$ orbital.[15] In the present case, where the overall spin state is $S = {}^3/_2$, the downfield-shifted average CH_2 resonance is fully consistent with a significant degree of internal reduction of the metal by the porphyrinate to create some degree of $S = 2$ Fe(II) antiferromagnetically coupled to an $S = {}^1/_2$ porphyrin radical, as was concluded above from the phenyl-H shift pattern.

For the [FeOETPP(4-CNPy)$_2$]ClO_4 complex, L 3,5-H and L 2,6-H resonances are characterized by large downfield shifts of 86.4 and 137.0 ppm at 183 K, respectively. These large downfield shifts are totally consistent with either the $S = 2$ Fe(II) state antiferromagnetically coupled to a porphyrinate radical, or the $S = {}^3/_2$ Fe(III) state, with half-occupation of the d_{z^2} orbital in either case, which allows significant σ-spin delocalization to the axial ligands, and downfield shifts.[15]

Thus, although the NMR spectra of [FeOETPP-(4-CNPy)$_2$]ClO_4 have previously been explained in terms of a simple $S = {}^3/_2$ iron porphyrinate,[9,10,20] we find that the chemical shifts of this complex are characterized by (i) large and negative phenyl-H shift differences $\delta_m - \delta_p$ and $\delta_m - \delta_o$, (ii) larger average CH_2 shifts than expected for the presence of either one or two unpaired electrons in π-symmetry d-orbitals, and (iii) large positive shifts of the 2,6-H and 3,5-H of the axial 4-CNPy ligands. The first (i) is indicative of negative spin density at the *meso*-carbons, the second (ii) is consistent with at least partial occupation of the $d_{x^2-y^2}$ orbital, and the third (iii) is consistent with occupation of the d_{z^2} orbital. These three facts lead to an overall electron configuration of the metal of $(d_{xy})^2(d_{xz},d_{yz})^2(d_{z^2})^1(d_{x^2-y^2})^{(1-x)}$ and of the porphyrin ring of $(OETPP)^{(2-x)-}$ with antiferromagnetic coupling of metal and ligand fractional electrons x. Whether $x = 1.0$ or less than 1.0 cannot be determined without additional experiments (for example magnetic Mössbauer studies) and theoretical, especially DFT, calculations.

In comparison to [FeOETPP(4-CNPy)$_2$]ClO_4, the chemical shifts for the methyl and α-methylene protons in the corresponding OMTPP and TC_6TPP complexes have strong negative temperature dependences, which indicate a change

(53) Buisson, G.; Deronzier, A.; Duée, E.; Gans, P.; Marchon, J.-C.; Regnard, J.-R. *J. Am. Chem. Soc.* **1982**, *104*, 6793−6795.
(54) Sakai, T.; Ohgo, Y.; Ikeue, T.; Takahashi, M.; Takeda, M.; Nakamura, M. *J. Am. Chem. Soc.* **2003**, *125*, 13028−13029.
(55) Zakharieva, O.; Schünemann, V.; Gerdan, M.; Licoccia, S.; Cai, S.; Walker, F. A.; Trautwein, A. X. *J. Am. Chem. Soc.* **2002**, *124*, 6636−6648.
(56) Schünemann, V.; Gerdan, M.; Trautwein, A. X.; Haoudi, N.; Mandon, D.; Fischer, J.; Weiss, R.; Tabard, A.; Guilard, R. *Angew. Chem., Int. Ed.* **1999**, *38* (21), 3181−3183.

from the $S = {}^3/_2$ state to LS as the temperature is lowered. In the pure LS state, with the $(d_{xz},d_{yz})^4(d_{xy})^1$ configuration, spin delocalization to the pyrrole-β position is negligible,[14,15] and as a result, the chemical shift of $CH_2(\alpha)$ in [FeTC$_6$TPP-(4-CNPy)$_2$]ClO$_4$ is in the diamagnetic region at low temperatures (6.8 ppm at 183 K). The methyl resonance in [FeOMTPP(4-CNPy)$_2$]ClO$_4$ is still shifted downfield (δ = 31.4 ppm at 183 K), indicating significant population of the $S = {}^3/_2$ state, even at this temperature. The nature of the $S = {}^3/_2$ state for these two complexes cannot be deduced with certainty because it is not possible to achieve fully the $S = {}^3/_2$ state. However, it should be noted that above 198 K the order of phenyl-H shifts of the [FeOMTPP(4-CNPy)$_2$]ClO$_4$ complex is the same as for [FeOETPP(4-CNPy)$_2$]ClO$_4$, suggesting that this complex also has some contribution from the $S = 2$ Fe(II) state antiferromagnetically coupled to an $S = {}^1/_2$ porphyrin π-cation radical.

Analysis of the temperature dependences of the resonances using our fitting program that includes the contributions of one or more thermally accessible excited states[39] shows that, despite the complications due to other temperature-dependent processes going on in the solution (ligand exchange kinetics, porphyrin ring inversion kinetics, hindered ethyl rotation at low temperatures), the phenyl-H resonances of [FeOETPP-(4-CNPy)$_2$]ClO$_4$ show linear 1-level temperature dependence, while the chemical shifts of both [FeOMTPP(4-CNPy)$_2$]ClO$_4$ and [FeTC$_6$TPP(4-CNPy)$_2$]ClO$_4$ below 198 K have temperature dependences that indicate an $S = {}^1/_2$ ground state and a thermally accessible $S = {}^3/_2$ excited state, with the excited-state being 650 cm^{-1} above the ground state for the former and 900 cm^{-1} for the latter. The temperature-dependent fits for these two complexes are shown in Supporting Information Figure S8A,B; in both cases, only the data below 198 K were used in the 2-level fit. The excited states in each case are much higher in energy than would be predicted on the basis of the full temperature dependence observed for these complexes, and the chemical shifts of all protons above 198 K clearly do not fit the 2-level plots. This is because of the onset of a *thermodynamic equilibrium* between the $S = {}^1/_2$ and $S = {}^3/_2$ states in each case, as was observed for the dependence of magnetic moment on temperature, Figure 5, which provides a much lower energy route for the change in spin state and therefore the observed temperature dependence of the ^{1}H NMR shifts. Thus, at higher temperatures than 198 K, first the OMTPP complex and then the TC$_6$TPP complex become involved in thermodynamic equilibria between the $S = {}^1/_2$ and the $S = {}^3/_2$ spin states, which dominate the chemical shifts of both of these complexes above 198 and 223 K, respectively. Similar behavior was found for the alkyl peroxide complex [FeTPP(OCH$_3$)(OO-*t*-Bu)]$^-$, where a thermodynamic equilibrium between the $(d_{xy})^2(d_{xz},d_{yz})^3$ and $(d_{xz},d_{yz})^4(d_{xy})^1$ electron configurations and, thus, likely also a planar and a ruffled porphyrinate ring was observed.[57]

The axial ligand 2,6-H and 3,5-H resonances in the pure LS [FeTC$_6$TPP(4-CNPy)$_2$]ClO$_4$ are shifted strongly upfield (−9.9 and −35.5 ppm at 183 K for L 3,5- and L 2,6-, respectively). The NMR results obtained for [FeOMTPP-(4-CNPy)$_2$]ClO$_4$ are in good agreement with the above data: L 3,5-H and 2,6-H have strong negative slope in the Curie plot (Figures S4A and S8A), indicating transition from $S = {}^3/_2$ (with downfield shifts for L) to $S = {}^1/_2$ (with upfield shifts for L) ground states as the temperature decreases.

In summary, as for the simple [FeTPP(4-CNPy)$_2$]$^+$ complex,[16] the LS state of the OMTPP and TC$_6$TPP complexes with $(d_{xz},d_{yz})^4(d_{xy})^1$ electron configuration is characterized by large and positive values of the phenyl-H shift differences $\delta_m - \delta_p$ and $\delta_m - \delta_o$ due to large $(+)\pi$ spin density at the *meso*-carbons. A small spin density at the pyrrole-β positions, on the other hand, results in chemical shifts for methyl or methylene protons in ORTPP complexes that are usually in the diamagnetic region. Ligated 4-CNPy has large upfield shifts for both of its proton resonances. Therefore, while EPR spectroscopy is a good probe for the electronic ground state at low temperatures, NMR spectroscopy is very useful in defining the spin state of the complex at ambient conditions, and for determining the nature of spin state behavior, whether it is due to a thermally accessible excited state or a thermodynamic equilibrium between spin states, or both.

Structures of the Complexes. The crystal structure data for [FeOMTPP(4-CNPy)$_2$]ClO$_4$ and [FeOETPP(4-CNPy)$_2$]-ClO$_4$ were obtained at 170 K. According to the solution magnetic measurements at this temperature, [FeOETPP-(4-CNPy)$_2$]ClO$_4$ exists as an $S = {}^3/_2$ state complex but [FeOMTPP(4-CNPy)$_2$]ClO$_4$ is largely LS with the $(d_{xz},d_{yz})^4$-$(d_{xy})^1$ electronic ground state; however, in the structures of all three complexes the Fe−N$_{ax}$ distances of about 2.2 Å are indicative of either the IS state or the HS Fe(II), $S = {}^1/_2$ cation radical with antiferromagnetic coupling. For the LS complexes of OMTPP and OETPP with various strong basicity pyridines and imidazoles (4-Me$_2$NPy, 1-MeIm, and 2-MeHIm)[18,42] (also see Table 2), the Fe−N$_{ax}$ distances are on average 2.0 Å, about 0.2 Å shorter than in the present case. For the admixed $S = {}^3/_2$, ${}^5/_2$ spin state of [FeOEP-(3,5-Cl$_2$Py)$_2$]ClO$_4$, the average Fe−N$_{ax}$ distance is even longer (2.347(4) Å) than for $S = {}^3/_2$ complexes.[3] Thus, there appears to be a correlation between the axial ligand bond length and the spin state of the complex: axial bond length increases as the spin state changes from the LS state (Fe−N$_{ax}$ ∼ 2.0 Å) through the $S = {}^3/_2$ state (Fe−N$_{ax}$ ∼ 2.2 Å) to the HS state (Fe−N$_{ax}$ > 2.3 Å).

The question arises as to why the [FeOMTPP(4-CNPy)$_2$]-ClO$_4$ complex is in the $S = {}^3/_2$ state rather than the LS state in the crystal lattice used for structure determination. It should be noted that all three sets of crystals were grown at room temperature, where [FeOMTPP(4-CNPy)$_2$]ClO$_4$ and [FeO-ETPP(4-CNPy)$_2$]ClO$_4$ complexes exist in the $S = {}^3/_2$ spin state (Figure 5). Freezing of the samples on the diffractometer was done in a cold stream of nitrogen over the course of a few seconds; therefore, it is quite likely that the room temperature geometry was trapped and preserved at 170 K. In the case of [FeOMTPP(4-CNPy)$_2$]ClO$_4$, it is possible that a spin transition may be seen if the sample is cooled slowly and to lower temperatures. A spin transition was detected in

(57) Rivera, M.; Caignan, G. A.; Astashkin, A. V.; Raitsimring, A. M.; Shokhireva, T. Kh.; Walker, F. A. *J. Am. Chem. Soc.* **2002**, *124*, 6077−6089.

$[FeOETPP(Py)_2]ClO_4$ by cooling the sample from 298 to 180 K and then to 80 K.[21] Most of the bonds contracted at lower temperatures, but the shortening of the axial bonds was the most prominent. The average $Fe-N_{ax}$ bond length decreased from 2.201(3) to 2.041 A and then to 1.993(3) Å.[21] This indicates that the spin state changed from $S = {}^3/_2$ to LS in the course of the X-ray experiments. In the solution magnetic susceptibility experiments, $[FeOMTPP(4\text{-}CNPy)_2]ClO_4$ behaves in the same manner as observed for $[FeOETPP(Py)_2]ClO_4$ in the solid state: the magnetic moment of both complexes decreases from ~3.6 μ_B at 300 K to ~2.8 μ_B at 200 K.[21] It would therefore be interesting to try variable temperature X-ray crystallographic experiments on $[FeOMTPP(4\text{-}CNPy)_2]ClO_4$. In contrast, $[FeOETPP(4\text{-}CNPy)_2]ClO_4$ is in the $S = {}^3/_2$ state at all temperatures achievable by X-ray experiments.

All complexes studied in this research have a predominantly saddled porphyrin core with estimated ruffling admixture ranging from 1% to 17% (see Table 3). Of course, the saddled distortion is stronger in any OETPP complex as compared to OMTPP, because the former has bulkier groups on the pyrrole β-positions. Stronger saddling is reflected in smaller dihedral angles of the phenyls, and a larger deviation of pyrrole β-C's from the mean porphyrin plane. In the structure of $[FeOMTPP(4\text{-}CNPy)_2]ClO_4$, the average dihedral angle of the phenyls is 48.0°, while in any of the $[FeOETPP(4\text{-}CNPy)_2]ClO_4$ structures it is not higher than 43°. The highest deviation of the porphyrin core atoms in $[FeOMTPP(4\text{-}CNPy)_2]ClO_4$ is 1.21 Å, which is substantially smaller than the highest deviation in $[FeOETPP(4\text{-}CNPy)_2]ClO_4$, **3**, 1.40 Å. A saddled distortion of the porphyrin core should require perpendicular orientation of the axial ligands; however in the case of $[FeOMTPP(4\text{-}CNPy)_2]ClO_4$ and $[FeOETPP(4\text{-}CNPy)_2]ClO_4$, **2**, much smaller dihedral angles are observed, 64.3° and 67.1°, respectively. To our knowledge these are the smallest observed "perpendicular" angles in octaalkyltetraphenylporphyrins with pyridine axial ligands, but these small angles are probably made possible by the much longer $Fe-N_{ax}$ bond lengths of the $S = {}^3/_2$ Fe(III) centers.

Due to the strongly saddled distortions, the $Fe-N_P$ distances are short (see Table 2). In general, OMTPP complexes should have longer distances than OETPP but shorter than TC_6TPP.[18] In this case, the $Fe-N_P$ distances in $[FeOMTPP(4\text{-}CNPy)_2]ClO_4$ are longer than those in $[FeOETPP(4\text{-}CNPy)_2]ClO_4$ structures **1**−**4** but almost the same as the $Fe-N_P$ distances in **5** and **6**.

Conclusions. Broadly speaking, most of the conclusions of this study are in agreement with those of the previous study:[10] $[FeOETPP(4\text{-}CNPy)_2]ClO_4$ exists as a complex with an overall spin state of $S = {}^3/_2$ at any temperature. This is reflected in the NMR, EPR, and magnetic susceptibility measurements, but the numerical data differ somewhat, as discussed above. At 4.2 K it also exhibits a low spin ($S = 1/2$) EPR signal ($g = 3.03$), suggesting that it is possible for some molecules to have the $(d_{xy})^2(d_{xz},d_{yz})^3$ electron configuration in frozen solution. However, there is no evidence in the temperature dependence of the ^1H NMR shifts for an $S = {}^1/_2$ ground state for the majority of molecules. In contrast to the previous study,[10] it has been shown herein that the NMR spectra (phenyl-H shifts) indicate that the actual electronic state involves a significant contribution from an $S = 2$ Fe(II) center antiferromagnetically coupled to an $S = {}^1/_2$ porphyrinate π-cation radical; however, the amount of this contribution has not been quantified. On the other hand, as also concluded previously,[10] $[FeOMTPP(4\text{-}CNPy)_2]ClO_4$ and $[FeTC_6TPP(4\text{-}CNPy)_2]ClO_4$ complexes exist as an equilibrium mixture of $S = {}^3/_2$ and LS spin states above 180 and 240 K, respectively, and at lower temperatures (4.2 K), they adopt a low spin $(d_{xz},d_{yz})^4(d_{xy})^1$ configuration. For two of the complexes, the rates of porphyrin ring inversion/axial ligand rotation could be measured, by NOESY/EXSY methods for $[FeOETPP(4\text{-}CNPy)_2]ClO_4$ and by dynamic NMR methods (DNMR) for $[FeTC_6TPP(4\text{-}CNPy)_2]ClO_4$. The results show that $[FeOETPP(4\text{-}CNPy)_2]ClO_4$ has a fairly low activation enthalpy (32 kJ mol^{-1}) and very negative activation entropy (−104 J mol^{-1} K^{-1}), leading to a rate constant of 59 s^{-1} in CD_2Cl_2 at 298 K. In comparison, for $[FeTC_6TPP(4\text{-}CNPy)_2]ClO_4$ the activation enthalpy is even lower (24 kJ mol^{-1}), the estimated activation entropy is less negative (at least −20 J mol^{-1} K^{-1}), and the estimated rate constant at the same temperature in the same solvent is at least 4.4×10^7 s^{-1}, about a million times faster than for $[FeOETPP(4\text{-}CNPy)_2]ClO_4$. These values attest to the much greater flexibility of the TC_6TPP ring. In the solid state, the $[FeOETPP(4\text{-}CNPy)_2]ClO_4$ and $[FeOMTPP(4\text{-}CNPy)_2]ClO_4$ complexes are mostly saddled with close to perpendicular ligand orientation. $Fe-N_{ax}$ bond lengths (~2.2 Å) indicate the $S = {}^3/_2$ state in both cases. In order to reach the spin transition for the $[FeOMTPP(4\text{-}CNPy)_2]ClO_4$ case, lower temperatures are required than were used for X-ray crystallography (170 K).

Acknowledgment. The support of the National Institutes of Health, Grant DK-31038 (F.A.W.), the National Science Foundation, Grant CHE9610374 (X-ray diffractometer grant), and the University of Arizona Molecular Structure Laboratory in this research are gratefully acknowledged. Dr. Michael D. Carducci, X-ray Facility specialist, Department of Chemistry, University of Arizona, is thanked for his help in structure refinement, and Dr. Charles F. Campana, from Bruker, is thanked for his help with the absorption corrections and refinement of the twinned structure of $[FeOETPP(4\text{-}CNPy)_2]ClO_4$ from $CDCl_3$/cyclohexane. Dr. Sheng Cai is thanked for his help in processing magnetic susceptibility data, Dr. Nikolai V. Shokhirev for fitting the ^1H NMR shifts to the 2-level temperature dependent fitting program, TDFw, and Professor Mario Rivera for providing very helpful comments. This paper was revised when F.A.W. was on Sabbatical leave at the Institute of Physics at the University of Lübeck with support from an Alexander von Humboldt Senior Research Award and is dedicated to Professor and Rector Alfred X. Trautwein on the occasion of his 63rd birthday.

Supporting Information Available: Details of the structure determinations, Figures S1−S8, and Tables S1−S19.This material is available free of charge via the Internet at http://pubs.acs.org.

IC035010Q